Sources of atmospheric aerosol from long-term measurements (5 years) of chemical composition in Athens, Greece

D. Paraskevopoulou [a,b], E. Liakakou [a], E. Gerasopoulos [a], N. Mihalopoulos [a,b,*]

[a] *Institute for Environmental Research and Sustainable Development, National Observatory of Athens, I. Metaxa and Vas. Pavlou, 15236, P. Penteli, Athens, Greece*
[b] *Environmental Chemical Processes laboratory (ECPL), Department of Chemistry, University of Crete, P.O. Box 2208, 71003 Heraklion, Greece*

HIGHLIGHTS

- First long-term continuous daily record of Athens' aerosol chemical composition.
- Study period includes years before and during the Greek economic recession.
- Identification and quantification of fine aerosol sources' contribution.
- Discrimination between regional and local emission sources.

ARTICLE INFO

ABSTRACT

To identify the sources of aerosols in Greater Athens Area (GAA), a total of 1510 daily samples of fine (PM$_{2.5}$) and coarse (PM$_{10-2.5}$) aerosols were collected at a suburban site (Penteli), during a five year period (May 2008–April 2013) corresponding to the period before and during the financial crisis. In addition, aerosol sampling was also conducted in parallel at an urban site (Thissio), during specific, short-term campaigns during all seasons. In all these samples mass and chemical composition measurements were performed, the latest only at the fine fraction. Particulate organic matter (POM) and ionic masses (IM) are the main contributors of aerosol mass, equally contributing by accounting for about 24% of the fine aerosol mass. In the IM, nss-SO$_4^{-2}$ is the prevailing specie followed by NO$_3^-$ and NH$_4^+$ and shows a decreasing trend during the 2008–2013 period similar to that observed for PM masses. The contribution of water in fine aerosol is equally significant (21 $\pm$ 2%), while during dust transport, the contribution of dust increases from 7 $\pm$ 2% to 31 $\pm$ 9%. Source apportionment (PCA and PMF) and mass closure exercises identified the presence of six sources of fine aerosols: secondary photochemistry, primary combustion, soil, biomass burning, sea salt and traffic. Finally, from winter 2012 to winter 2013 the contribution of POM to the urban aerosol mass is increased by almost 30%, reflecting the impact of wood combustion (dominant fuel for domestic heating) to air quality in Athens, which massively started in winter 2013.

© 2015 Elsevier B.V. All rights reserved.

1. Introduction

Aerosols constitute a significant component of the atmospheric system. They are emitted in the atmosphere by variable sources, through diverse formation and subsequent transformation mechanisms, resulting in a mixture of chemical characteristics. Particulate matter is of the most highlighted atmospheric pollutants, due to its effect on local and regional deterioration of air quality, visibility reduction (Kanakidou et al., 2005) and global climate system (Seinfeld and Pandis, 1998).

Aerosols aerodynamically smaller than 2.5 μm (PM$_{2.5}$) are of particular concern because of the significant contribution to detrimental health effects (Dockery and Pope, 1994; Ostro et al., 2006), since they act as carriers for toxicants and mutagenic components (Beddows et al., 2004) and, owing to their size, are able to penetrate cell membranes (Li et al., 2003), permeating easier into human organism (Salma et al., 2002; Bell et al., 2009). As a consequence, one of the major challenges in aerosol science is the knowledge of fine particle chemical properties and the identification and quantification of emission sources at local and regional scales.

The city of Athens is situated in the Mediterranean Basin, which constitutes a crossroad of three continents, being highly influenced by ambient particles with both natural and anthropogenic origin deriving from marine boundary layer, Saharan desert and European mainland (Gerasopoulos et al., 2011; Perrone et al., 2011; Bougiatioti et al.,

* Corresponding author at: Institute for Environmental Research and Sustainable Development, National Observatory of Athens, I. Metaxa and Vas. Pavlou, 15236, P. Penteli, Athens, Greece.
E-mail address: mihalo@chemistry.uoc.gr (N. Mihalopoulos).

2013). Several studies have focused on PM$_{2.5}$ concentration levels and composition, in Athens, during sampling periods of a few months to one year (e.g., Sillanpää et al., 2006; Karageorgos and Rapsomanikis, 2007; Theodosi et al., 2011; Pateraki et al., 2012; Remoundaki et al., 2013; Kassomenos et al., 2014); some of which included a chemical mass closure exercise. Nevertheless, the source identification and apportionment of particulate matter is more appropriately attained through a combination of source apportionment tools including Positive Matrix Factorization (PMF) (Belis et al., 2013 and references therein). This kind of source apportionment technique is rare in Athens, Greece (Karanasiou et al., 2009; Mantas et al., 2014) and relatively recent in the Eastern Mediterranean Basin, being reported by a limited number of authors (Kocak et al., 2009; Kocak et al., 2011; Ozturk et al., 2012).

The present paper uses for the first time, to our knowledge, an uninterrupted 5-year daily sampling dataset in Penteli, which constitutes a regional suburban site, in order to perform a chemical mass closure exercise, including carbonaceous materials, ionic species and, for a selected number of samples trace metals. The inter-annual trends (from 2008 to 2013) of the analyzed species are studied, in order to investigate the effects of the economic crisis on the quality of the air. Furthermore, all the acquired data are analyzed through a variety of source apportionment techniques including chemical mass closure, principal component analysis (PCA) and PMF to identify the sources of fine aerosols at the studied suburban site in Athens and determine the contribution of each source to PM$_{2.5}$ mass on a five-year basis. Additionally, four campaigns with simultaneous measurements at the suburban station (Penteli) and an urban site (Thissio) were performed. Based on the differences between the two sites, the relative contribution of regional and local aerosol sources is quantified. PMF analysis is applied for the first time on a long-term data set, while concurrent characterization of local and regional aerosol sources is performed. Additionally, in parallel with the investigation of the inter-annual variability of air pollutant levels over Athens, the acquired PMF results are compared to posterior (prior to economic crisis i.e., 2008) PMF analysis performed for the studied area, in order to reach to more secure results regarding the impacts of the economic crisis on the air quality of Athens as, during the last years (2008 and onwards), a new era characterized by intense wood burning for domestic heating has begun.

2. Methodology

2.1. Sampling sites

The implementation of this analysis is based on the operation of two ground based stations in Athens. Penteli station (38° 2.94′ N, 23° 51.78′ E, 495 m a.s.l.) is located at 17 km from the center of Athens in a suburban location, within the premises of the National Observatory of Athens at Penteli (Fig. 1). A detailed description of the sampling site is provided by Paraskevopoulou et al. (2014). The second station is at the National Observatory of Athens premises at Thissio (38° 0.00′ N, 23° 43.48′ E, 110 m a.s.l.), located on top of a hill down-town Athens, surrounded mostly by a pedestrian zone and populated neighborhoods, while to the S–SE sector it adjoins with the Filopappou and Acropolis Hills (Fig. 1). Thissio station, located in the historical center of Athens, is considered an urban station which reflects the average pollution of the city. The major sources of air pollution affecting the two sites at different degrees, are expected to be vehicular emissions and residential heating. A detailed description of the Athens' morphology, meteorology and dominant transport patterns is provided by Kanakidou et al. (2011) and Melas et al. (1998) and references therein.

2.2. Sampling and mass measurement

A total of 1510 samples of fine and separately of coarse aerosols were collected at the Penteli site, during a five year period (May 2008–April 2013), on quartz fiber filters (4.7 cm, Whatman QMA). The collection was conducted using a Dichotomous Partisol sampler (R&P Co) during most of the period (90% of the sampling time) and a Partisol FRM Model 2000 PM$_{2.5}$ & PM$_{10}$ air samplers (R&P Co) (10% of the sampling time). A detailed overview of the sampling and the applied samplers is given by Paraskevopoulou et al. (2014).

Parallel aerosol collection was also conducted at Thissio during specific, short-term campaigns, in order to identify and discriminate between local and regional aerosol sources and contribution. Overall, four experimental campaigns were organized during different seasons of the year: from 28 June to 1 August 2011 (summer campaign), from 16 January to 17 February 2012 (winter campaign), from 9 March to 5 April 2012 (spring campaign) and from 11 January to 8 February 2013
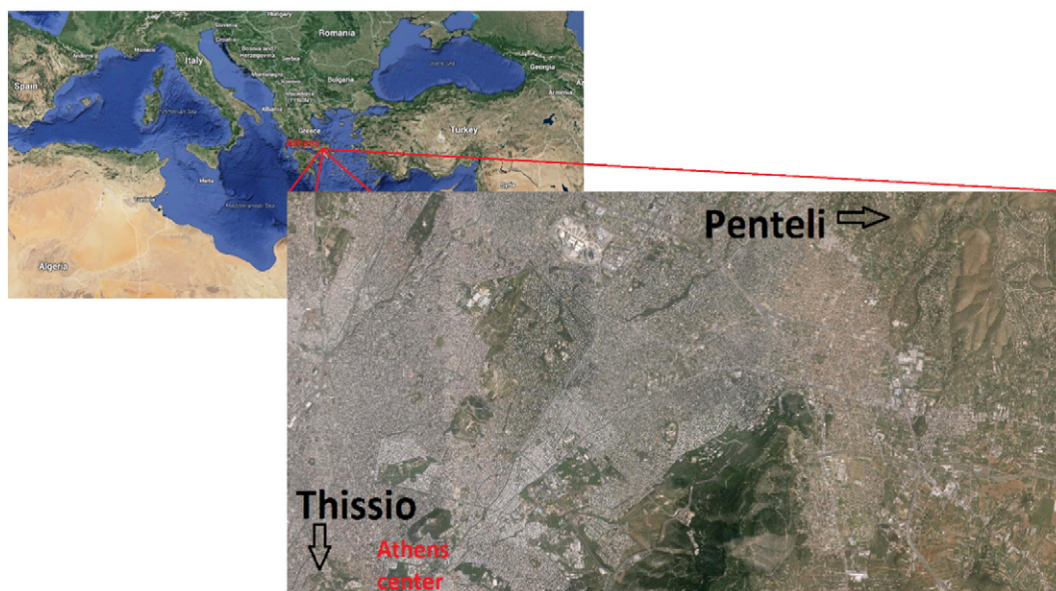

Fig. 1. Map indicating the sampling sites at Thissio (urban location) and Penteli (suburban location).

(2nd winter campaign, characterized by intense wood burning for domestic heating). These campaigns led to the collection of 210 samples of fine and separately of coarse aerosols. During all four campaigns, the particulate matter collection was conducted with a Dichotomous Partisol sampler (R&P Co) using 4.7 cm quartz fiber filters (Whatman QMA).

The sampling duration was typically 24 h at the Penteli suburban site, while at Thissio it was 24 h from summer 2011 until spring 2012 and 6 h in winter 2013. Filter handling was identical for both sites and is described in detail by Paraskevopoulou et al. (2014). Briefly, the utilized filters were pre-combusted at 550 °C before sampling while; after aerosol collection, the samples along with the treated blanks were stored until analysis. Each filter was used for determination of gravimetric aerosol mass concentration following the US EPA RFPS-1298-126 method and using a Mettler Toledo MX5 microbalance, according to the procedure reported by Paraskevopoulou et al. (2014).

2.3. Analytical techniques

All PM$_{2.5}$ collected samples were analyzed for organic and elemental carbon and for major ions while, a selected number of fine aerosol samples were analyzed for trace and major elements, as well. Organic (OC) and elemental carbon (EC) concentrations were measured with a Sunset Laboratory Inc. (Oregon) carbon analyzer using the EUSAAR-2 protocol (Cavalli et al., 2010). Punches of 2 cm^2 from each filter were analyzed by ion chromatography for the major anions (Cl$^-$, Br$^-$, NO^{-3}, SO$_4^{-2}$ and C$_2$O$_4^{-2}$) and cations (NH$_4^+$, K$^+$, Na$^+$, Mg^{+2} and Ca^{+2}). Analytical procedures for ion analysis are reported in detail by Paraskevopoulou et al. (2014). With regard to the elemental analysis, 2 cm^2 of each quartz filter was acid digested through a microwave procedure, as described by Theodosi et al. (2010). Briefly, the samples were placed in Teflon vessels (DAP-60 K, 60 mL/40 bar) along with concentrated nitric acid, in order to be processed in a Microwave digestion system (Berghof MWS-2) under controlled conditions. The acquired solutions were cooled to room temperature and were stored into acid-cleaned polyethylene containers, in order to be further analyzed by Inductively Coupled Plasma Optical Emission Spectrometry (ICP-OES, Thermo Electron ICAP 6000 Series) for major and trace metal concentrations. Indium (In, CPI International) was added as an internal standard to the samples before ICP-OES analysis. The detection limits of the analysis are reported for every element separately; Al: 0.12 µg L^{-1}, As: 1.43 µg L^{-1}, Ca: 0.003 µg L^{-1}, Cd: 0.07 µg L^{-1}, Cr: 0.21 µg L^{-1}, Cu: 0.39 µg L^{-1}, Fe: 0.25 µg L^{-1}, K: 0.60 µg L^{-1}, Mn: 0.07 µg L^{-1}, Na: 0.37 µg L^{-1}, Ni: 0.36 µg L^{-1}, P: 1.55 µg L^{-1}, Pb: 1.06 µg L^{-1}, S: 1.05 µg L^{-1}, Ti: 0.30 µg L^{-1}, V: 0.23 µg L^{-1} and Zn: 0.19 µg L^{-1}. All reported concentrations were corrected for blanks.

2.4. Data analysis

Multivariate statistical methodologies, including correlation coefficients, principal component analysis (PCA) (Blifford and Meeker, 1967) and Positive Matrix Factorization (PMF) (Paatero, 1997) were applied, to decompose the available, long term aerosol data set.

In particular, PCA was used to identify the sources of particulate matter in the atmosphere (e.g., Harrison et al., 1997). The statistical analysis was applied on PM$_{2.5}$ data being subjected to Varimax normalized rotation. PCA is a statistical procedure that is applied to smoothen the data set diversity by grouping the chemical species into principal components (eigenvectors). In order to weight each major, minor and trace species equally, the concentration of each specie was normalized to the species means (Engelhart et al., 2011), before applying PCA. During the analysis, the factors were determined by including some important chemical markers (e.g., particulate organic matter), explaining and representing each source characteristics of fine aerosol.

The application of regression analysis (correlation coefficients) and PCA provided us with a first step assessment tool for the selection of the chemical species to be considered for subsequent PMF source attribution modeling. The dataset was then processed with the PMF version of the United States Environmental Protection Agency (US-EPA) known as EPA PMF3.0, according to Norris et al. (2008). Missing data were replaced by the median value of the respective species and the corresponding uncertainty was calculated as four times the median concentration. Values below the Method Detection Limit (MDL) were substituted by MDL/2, given an uncertainty of 5/6 of the MDL (Polissar et al., 1998). Species with more than 95% of the values below MDL were not included in the dataset for PMF analysis, while those with signal-to-noise ratio smaller than 2 were excluded as well (Paatero and Hopke, 2003).

The combination of all criteria resulted in a 1223 × 10 matrix (1223 days × 10 species) that was finally deployed to identify aerosol sources. 13% extra modeling uncertainty was chosen and the PM$_{2.5}$ mass concentration was incorporated as the total variable. A total of 20 random runs were performed. The minimum Q value from the different runs was selected to carry out further analysis with PMF3.0 (Norris et al., 2008). Subsequently, 100 bootstrap runs were performed, with a minimum r^2-value of 0.6. that resulted to the mapping of all 6 factors to a base run, hence confirming the stability of the PMF solution.

Finally, air mass origins for the whole period of filter samplings, were identified by applying a 4-day back-trajectory analysis, with the Hybrid Single-Particle Lagrangian Integrated Trajectory (HYSPLIT) model (version 4.9) (Draxler et al., 2009), in order to classify all collected samples into dust and non-dust cases. The model uses the meteorological data produced by the National Weather Service's National Centers for Environmental Prediction (NCEP) from the Global Data Assimilation Group (GDAS), in order to compute advection and dispersion of air-parcels arriving over the sampling site.

3. Results and discussion

3.1. Particulate matter masses

The 24-h concentrations of PM$_{2.5}$, PM$_{2.5-10}$ and PM$_{10}$ at the suburban site at Penteli (Fig. 2 a, c, e) vary from 1.2 to 65.8 µg m^{-3}, 0.2 to 213.1 µg m^{-3} and 3.0 to 329.7 µg m^{-3}, respectively, with an overall average of 20 ± 11 µg m^{-3} for PM$_{2.5}$, 17 ± 13 µg m^{-3} for PM$_{2.5-10}$ and 35 ± 20 µg m^{-3} for PM$_{10}$. The annual average PM$_{2.5}$ and PM$_{10}$ masses are within the target and limit values imposed by the Air Quality Directive (2008/50/EC). In fine and coarse aerosols about 23% and 29% of values are above 25 and 40 µg m^{-3}, respectively, while, about 23% and 34% of these exceedances are attributed to dust cases for fine and coarse, respectively. High levels of PM masses, observed in Fig. 2, are attributed to dust events and intense fuel combustion due to domestic heating and vehicle emissions. Prior studies on aerosols, performed during shorter time intervals in Athens and in other Mediterranean cities, indicate similar or higher PM$_{2.5}$ and PM$_{10}$ levels (Table 1), depending on the site type and the different reference periods.

The relationship between daily fine and coarse levels is moderate (R = 0.56, n = 1130, p < 0.001), indicating that fine and coarse particles could be controlled by common sources and/or processes (Putaud et al., 2010; Perrone et al., 2011). The PM$_{2.5}$/PM$_{10}$ ratio for the whole studied period is 0.60 ± 0.21, in agreement with the ratios reported by Theodosi et al. (2011) (0.58 for remote background site) and by Chaloulakou et al. (2005) (0.53), highlighting, hence, the importance of fine aerosol fraction in the levels of ambient particulate matter. The analysis of seasonal data points out peaks of PM$_{2.5}$ and PM$_{10}$ aerosol masses during the coldest period of the year and on periods of dust transport from North Sahara (Fig. 2b, d, f). In order to study the inter-annual trend of PM masses, the mean annual mass concentrations were calculated from the daily gravimetrically measured masses, revealing thus a decrease of ambient aerosol masses (p < 0.05) through the studied 5-year period (Fig. 3). In particular, PM$_{2.5}$ and PM$_{10}$ masses decrease respectively, from 32 ± 19 µg m^{-3} and 59 ± 21 µg m^{-3} in 2008, to 15 ± 6 µg m^{-3}
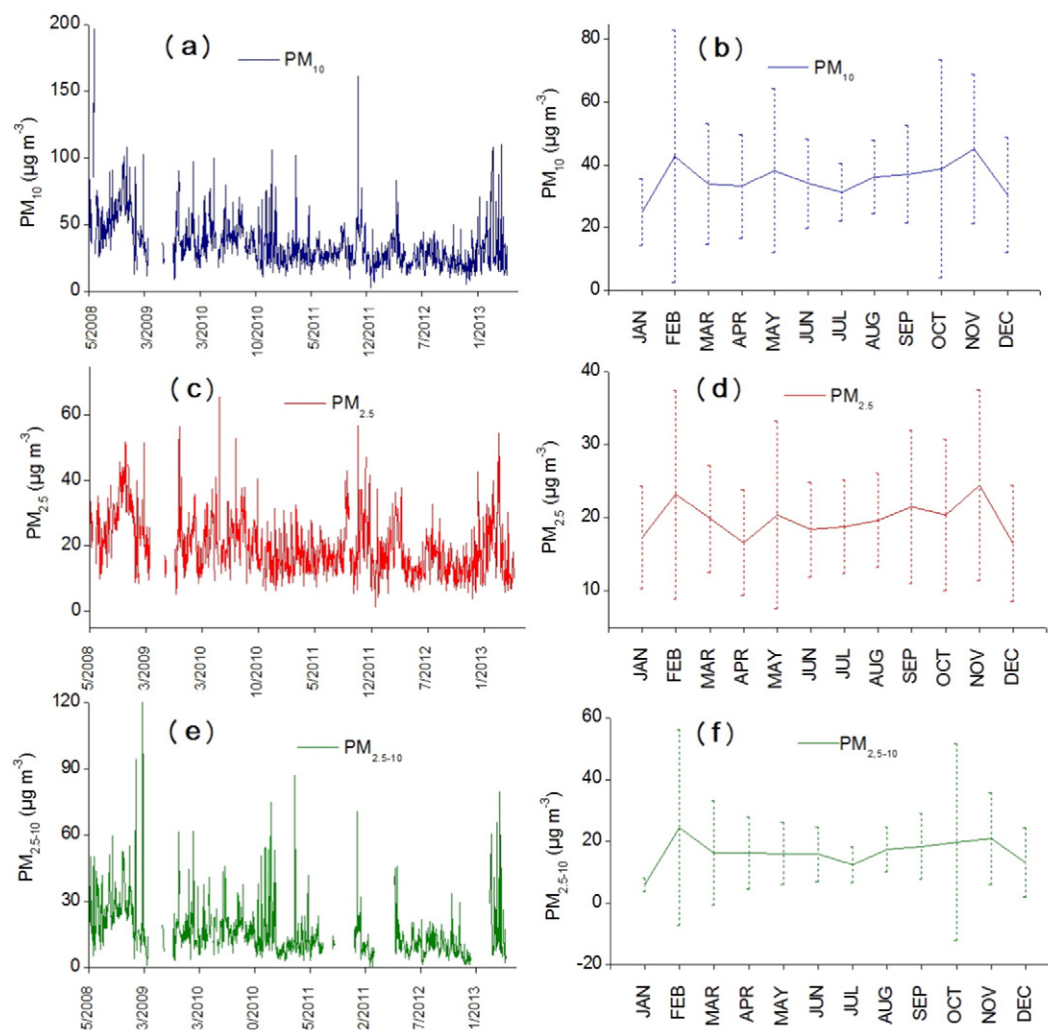
Fig. 2. Daily concentrations (a, c, e) and average seasonal cycles (b, d, f) of $PM_{2.5}$, $PM_{2.5–10}$ and PM_{10} mass concentrations at Penteli station for the period of May 2008–April 2013.

and $25 \pm 9 \, \mu g \, m^{-3}$ in 2012, marking a reduction of about 52% for $PM_{2.5}$ and about 58% for PM_{10} along the sampling period. It should be noted that $PM_{2.5–10}$ masses (not shown here) also present a reduction of 64% from 2008 to 2012. These results are in agreement with the general decline of pollution levels in the area (Kanakidou et al., 2011), after measures adopted during the last decades but also due to further reduction of anthropogenic emissions since the economic recession originating in Greece. A relevant analysis by Vrekoussis et al. (2013) showed that the reduction of air pollutants was actually accelerated during the economic crisis in the studied area. Recent Mediterranean studies have also reported a decrease in fine aerosol levels at regional stations (Viana et al., 2008a; Cusack et al., 2012; Kassomenos et al., 2014).

3.2. Organic and elemental carbon

A total of 1507 daily $PM_{2.5}$ samples were analyzed for their content in organic (OC) and elemental carbon (EC). The OC, EC and particulate organic matter (POM) levels, variability and controlling factors are described in detail by Paraskevopoulou et al. (2014). Briefly, average OC and EC concentration for the whole studied period is $2.1 \pm 1.3 \, \mu g \, m^{-3}$ and $0.54 \pm 0.39 \, \mu g \, m^{-3}$, respectively, and they present similar variability suggesting that OC and EC fractions (R = 0.7, slope = 2.33, n = 1365, p < 0.001) are emitted by common primary sources, at a regional scale. An average OC/EC ratio of 4.7 ± 1.3 is calculated, revealing a predominant secondary origin of OC, which is expected for

sites affected by long-range transport or under stagnant weather conditions.

On a seasonal basis, higher carbonaceous aerosol concentrations are observed in winter, since during the coldest period of the year, there is intense fuel combustion due to domestic heating. Paraskevopoulou et al. (2014) reported that in winter OC and EC mainly derive from local sources ($67 \pm 7\%$ of OC and $71 \pm 8\%$ of EC) such as fuel combustion (domestic heating), whereas during summer, the prevailing role of regional sources is maximized ($67 \pm 7\%$ of OC and $53 \pm 12\%$ of EC). Additionally, EC during summertime decreases throughout the years, since there is a simultaneous reduction in traffic due to the economic crisis in Greece. On the contrary, EC concentration during winter presents a noticeable increase since 2011, which is mainly attributed to the selection of wood as the major fuel source for domestic heating (Saffari et al., 2013; Paraskevopoulou et al., 2014).

3.3. Ionic composition

3.3.1. Levels of water soluble ions

Ion mass concentrations were classified into sea-salt (ss) and non-sea salt (nss), to discriminate sea spray contribution. Non-sea salt concentrations were estimated based on a standard sea water composition (Seinfeld and Pandis, 1998) and following the procedure described by Sciare et al. (2005) and Pio et al. (2007).

A detailed analysis of the ion mass fraction (not shown here) reveals that nss-SO_4^{-2} is the prevailing specie and, NO_3^- and NH_4^+ contribute to a

Table 1
PM$_{2.5}$, PM$_{2.5–10}$ and PM$_{10}$ mass concentrations reported in bibliography, compared to this study.

City	Site[a]	Sampling period	PM$_{2.5}$ µg m^{-3}	PM$_{2.5–10}$ µg m^{-3}	PM$_{10}$ µg m^{-3}
Athens[b]	Suburban	5/2008–4/2013	20 ± 11	17 ± 13	35 ± 20
Athens[c]	Urb-BG	2/6–21/7/2003	25.5	29.6	55.2
Athens[d]	Suburban	29/2–2/5/2008 4/6–5/8/2008	23.8	–	–
Athens[e]	Urban	2–12/2010	20	–	–
Athens[f]	Downtown	9/2005–8/2006	23.5 & 29.4	–	–
Athens[g]	Urb-BG	Winter 2005	14.66	–	22.69
	Urb-BG	Summer 2005	22.73	–	32.55
	Traffic	Winter 2005	32.47	–	44.13
	Traffic	Summer 2005	38.48	–	51.22
Thessaloniki[h]	Urb-Ind	12/2006–03/2007	–	–	69
	Urb-Ind	6–9/2009	–	–	58
	Urb-Tra	12/2006–03/2007	–	–	51
	Urb-Tra	6–9/2009	–	–	42
Finokalia[i]	Coastal	7/2004–7/2006	–	–	36
Lecce[j]	Urb-BG	3–12/2007	25	–	–
Milan[k]	Urb-BG	8/2002–12/2003	40	–	–
Madrid[g]	Urb-BG	Winter 2005	14.30	–	29.06
	Urb-BG	Summer 2005	13.49	–	34.50
	Traffic	Winter 2005	24.14	–	37.46
	Traffic	Summer 2005	20.63	–	38.87

[a] Urb-BG: Urban background, Urb-Ind: Urban industrial, Urb-Tra: Urban traffic.
[b] Current study.
[c] Pennanen et al. (2007).
[d] Pateraki et al. (2012).
[e] Remoundaki et al. (2013).
[f] Theodosi et al. (2011).
[g] Titos et al. (2014).
[h] Terzi et al. (2010).
[i] Koulouri et al. (2008).
[j] Perrone et al. (2011)
[k] Lonati et al. (2005).

lesser extent. These results are in agreement with posterior studies performed in Athens (Karageorgos and Rapsomanikis, 2007; Remoundaki et al., 2013; Mantas et al., 2014). The contribution of nss-SO$_4^{-2}$ to ionic mass (IM) is 63 ± 7% and 52 ± 14% for non-dust and dust samples, respectively, while with regards to the total PM$_{2.5}$ mass, nss-SO$_4^{-2}$ presents an average contribution of 15 ± 4% for the five-year period, which is within the range reported by Putaud et al. (2010) (12–21%) over Europe.

The time series of water soluble ions are presented in Fig. 4(a, c, e, g). The five year average mass concentration of SO$_4^{-2}$ is 3.1 ± 0.8 µg m^{-3}; and the highest and lowest daily values are 10.4 µg m^{-3} and 0.1 µg m^{-3}, respectively. The daily concentration levels of NH$_4^+$ vary from 0.01 µg m^{-3} to 3.82 µg m^{-3}, with an average of 0.67 ± 0.26 µg m^{-3}. Accordingly, the concentrations of NO$_3^-$ vary from 0.01 µg m^{-3} to 3.79 µg m^{-3} and the average is 0.45 ± 0.19 µg m^{-3}.
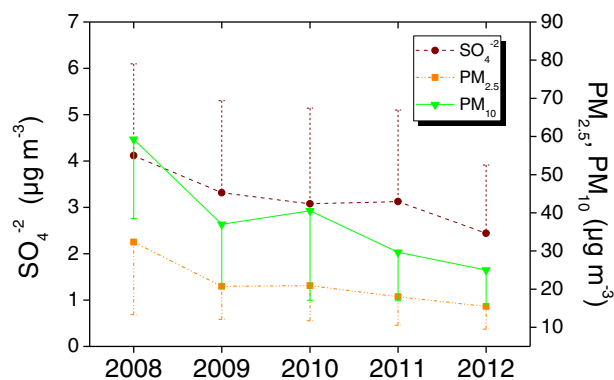

Fig. 3. Average annual concentrations of PM$_{2.5}$, PM$_{10}$ and SO$_4^{-2}$, calculated from daily values for the period of May 2008–April 2013.

The five-year average daily concentrations of Na$^+$, K$^+$, Ca^{+2}, Cl$^-$ and C$_2$O$_4^{-2}$ are 0.16 ± 0.02 µg m^{-3}, 0.18 ± 0.04 µg m^{-3}, 0.37 ± 0.11 µg m^{-3}, 0.16 ± 0.05 µg m^{-3}, and 0.18 ± 0.05 µg m^{-3}, respectively. The daily concentration levels of Mg^{+2} (average 0.03 ± 0.01 µg m^{-3}) are generally very low (<1 µg m^{-3}) during this long-term sampling period. All the reported mean concentrations of the studied ions are similar or lower than those reported for PM$_{2.5}$, during posterior studies conducted in Athens over shorter time periods and for different station types (Theodosi et al., 2011; Pateraki et al., 2012; Remoundaki et al., 2013).

3.3.2. Seasonal variability

On a seasonal basis, the highest nss-SO$_4^{-2}$ values are observed in late summer (average 3.05 ± 0.78 µg m^{-3}) and the lowest in winter (average 1.90 ± 0.31 µg m^{-3}) (Fig. 4b). Higher summer sulfate levels are the result of enhanced photochemistry associated with more intense solar radiation, combined with less precipitation and higher regional transport, favoring the regional mixing of polluted air masses (Cusack et al., 2012). Similar monthly distribution pattern is followed by NH$_4^+$ (Fig. 4f) that presents summer and winter averages of 1.02 ± 0.14 µg m^{-3} and 0.37 ± 0.05 µg m^{-3}, respectively. On the contrary, nitrate presents higher values in the coldest period (Fig. 4d, average: 0.55 ± 0.04 µg m^{-3}), potentially originating from local pollution sources, such as vehicular traffic and combustion for heating purposes. In addition the lower temperatures (average ~8 °C) encountered during this season favor stability of ammonium nitrate formed from subsequent reaction of NO$_3^-$ with NH$_4^+$ (Park et al., 2005; Mariani and de Mello, 2007), whose correlation improves significantly during the coldest period of the year (details provided in the following paragraphs). In summer, lower nitrate values (average: 0.23 ± 0.07 µg m^{-3}) are attributed to the thermal instability of ammonium nitrate (Harrison and Pio, 1983; Seinfeld and Pandis, 1998; Querol et al., 2004; Lonati et al., 2005), which is strongly influenced by high temperatures (average ~24 °C) that tend to dissociate fine mode nitrate into nitric acid and ammonia (Ho et al., 2006; Sillanpää et al., 2006; Theodosi et al., 2011), resulting in the seasonal variability of nitrate presented in Fig. 4d. In winter, nitrate accounts for about 3% of the PM$_{2.5}$ mass while in summer it accounts for about 1%. On the contrary, sulfate and ammonium contributions are larger in the warm season indicating that the possibility of forming ammonium nitrate should be very low or null during this season: sulfate accounts for 11% of PM$_{2.5}$ mass in winter and for 20% in summer; corresponding values for ammonium are 2% and 5%, respectively. Winter peaks for nitrate have already been reported for PM$_{2.5}$ in Athens by Sillanpää et al. (2006). Overall, the aforementioned seasonal variability of major ions, is in agreement with findings from other studies in Europe and the Eastern Mediterranean particularly (Sillanpää et al., 2006; Koulouri et al., 2008; Theodosi et al., 2011; Pateraki et al., 2012). It has to be noted that the inter-annual trend of nss-SO$_4^{-2}$ follows the decreasing trend of PM masses (Fig. 3). These lower levels of in-situ measured pollutants, as derived from detail chemical composition data, are reported for the first time in the area of Athens, highlighting the effects of the economic recession in Greece, such as industrial activities' suppression, reduction of traffic and behavioral changes regarding domestic heating. Similar results were reported by Vrekoussis et al. (2013) based on satellite observations over Athens for NO$_2$ and SO$_2$, the latter being the precursor of SO$_4^{-2}$. Vrekoussis et al. (2013) explained the observed decrease based on the economic crisis in Greece (from 2008 and onward) that resulted in a reduction of anthropogenic activities emitting gaseous pollutants to the atmosphere.

Na$^+$, nss-K$^+$, and Cl$^-$ show no obvious seasonal variability (not shown here). Unlike these ions, nss-Ca^{+2} is distinctly higher in spring and early fall (Fig. 4h), when fugitive dust from Sahara is present in the ambient air of the Eastern Mediterranean. For C$_2$O$_4^{-2}$ (not shown here), higher values are observed during summer (summer average: 0.25 ± 0.07 µg m^{-3}, winter average: 0.14 ± 0.01 µg m^{-3}), due to enhanced photochemistry and increased volatile organic compounds' (VOCs) emissions (Theodosi et al., 2011).
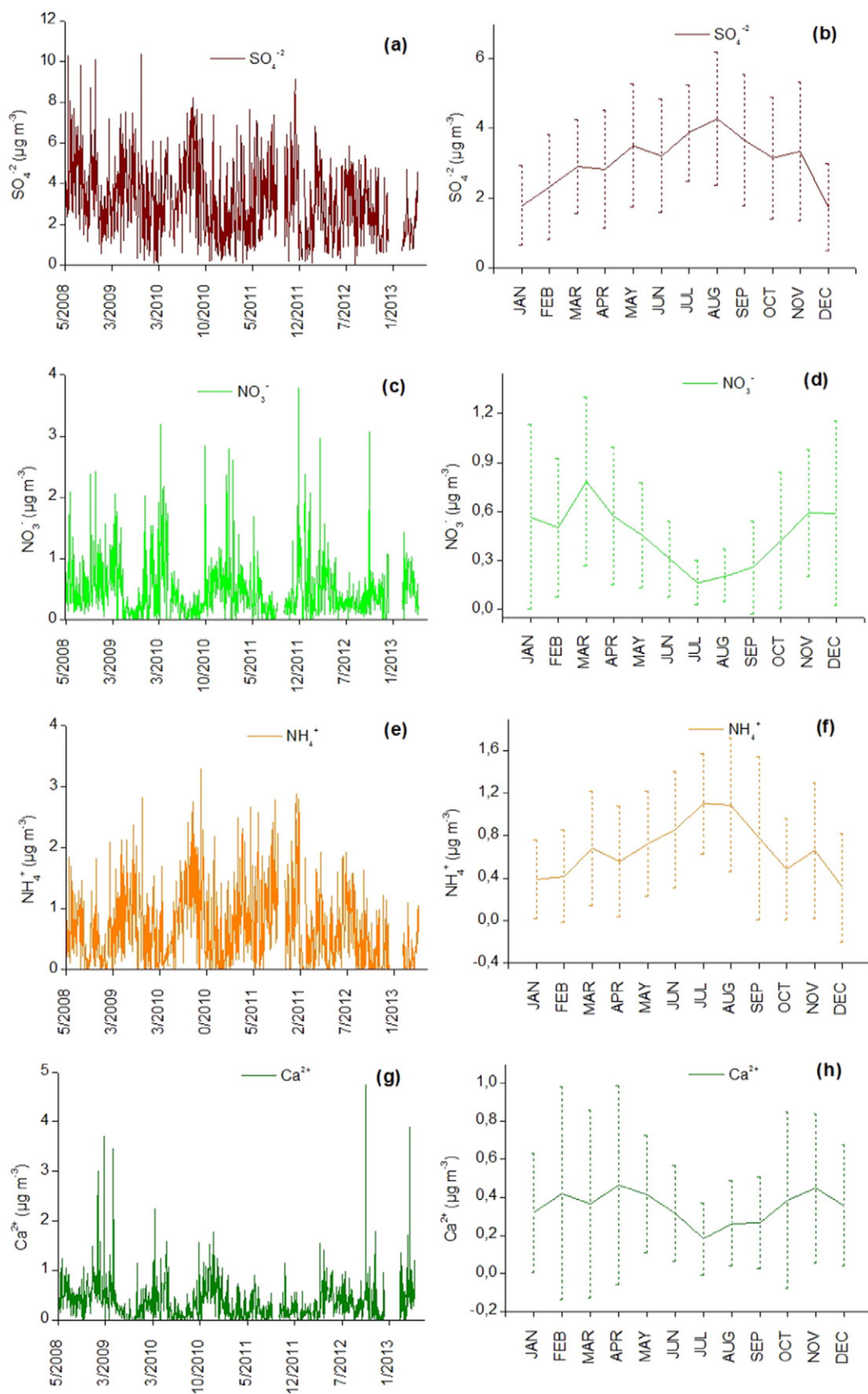
Fig. 4. Daily concentrations (a, c, e, g) and average seasonal cycles (b, d, f, h) of nss-SO_4^{-2}, NO_3^-, NH_4^+ and nss-Ca^{2+} at Penteli station, for the period of May 2008–April 2013.

Table 2
Regression analysis among daily values of different chemical species in PM$_{2.5}$ from May 2008 to April 2013.

Species	Correlation coefficient	p	n
NH$_4^+$ vs nss-SO$_4^{-2}$	0.83	<0.001	1393
C$_2$O$_4^{-2}$ vs nss-SO$_4^{-2}$	0.59	<0.001	1390
NH$_4^+$ vs C$_2$O$_4^{-2}$	0.57	<0.001	1424
PM$_{2.5}$ vs nss-SO$_4^{-2}$	0.50	<0.001	1285
OC vs C$_2$O$_4^{-2}$	0.47	<0.001	1362
NO$_3^-$ vs EC	0.43	<0.001	1359
PM$_{2.5}$ vs NH$_4^+$	0.36	<0.001	1317
OC vs nss-SO$_4^{-2}$	0.35	<0.001	1337
NO$_3^-$ vs NH$_4^+$	0.06	<0.05	1434
NO$_3^-$ vs nss-SO$_4^{-2}$	0.002	0.9	1400

The origin of major ions is investigated by examining the correlations among the different chemical species in fine aerosols (Table 2). Daily concentrations of NH$_4^+$ and nss-SO$_4^{-2}$ exhibit statistically significant correlation for the entire sampling period (no differentiation between warm and cold period), indicating the predominance of nss-SO$_4^{-2}$ as ammonium salt in the PM$_{2.5}$ fraction (Zhang et al., 2013), formed by photochemical reactions of ammonia with sulfuric acid (Daher et al., 2013). The slope is below unity (0.27 ± 0.004), indicating that sulfates are usually not sufficiently neutralized by NH$_4^+$ and could be, hence, associated with H$^+$ (see also below in Section 3.3.3). Similar results for the Eastern Mediterranean have been also reported by Bardouki et al. (2003) and (Koulouri et al., 2008) and, specifically for Athens, by Siskos et al. (2001) and Theodosi et al. (2011). Interestingly, it is observed all year round that NO$_3^-$ does not correlate with nss-SO$_4^{-2}$, which is another specie of anthropogenic origin. Nitrate, as explained earlier, displays elevated concentrations during the colder months of the year. Therefore, in contrast to summer (R = 0.2, n = 337, p < 0.001), nitrate is better correlated to ammonium in winter (winter R = 0.42, n = 283, p < 0.001), when there is indicative formation of ammonium nitrate. These correlations confirm the assumption that formation of NH$_4$NO$_3$ can occur to a certain extend during wintertime in agreement with Remoundaki et al. (2013) and Karageorgos and Rapsomanikis (2007). Furthermore, NO$_3^-$ presents a better correlation with EC during winter (winter R = 0.48, n = 274, p < 0.001, summer R = 0.30, n = 330, p < 0.001), revealing the primary and traffic-oriented origin of NO$_3^-$, even at an urban background site, in agreement with Mirante et al. (2014). The daily values of NH$_4^+$ and C$_2$O$_4^{-2}$ present a statistically significant correlation (R = 0.57, n = 1424, p < 0.001) that depicts some year round common secondary sources, namely photochemistry and heterogeneous chemistry.
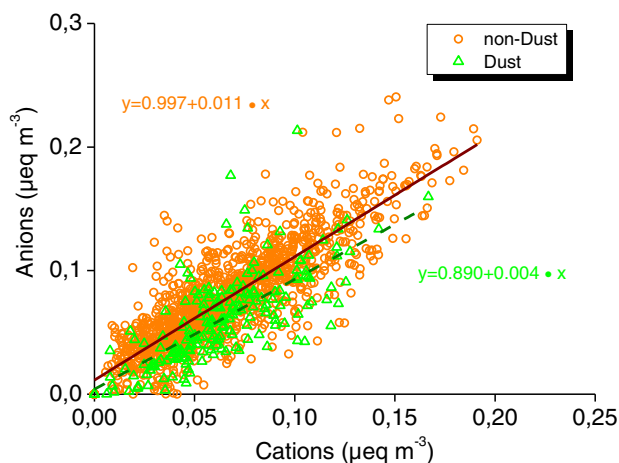
A good correlation is also found between C$_2$O$_4^{-2}$ and nss-SO$_4^{-2}$ (R = 0.59, n = 1390, p < 0.001); the latter being typically emitted by anthropogenic activities via heterogeneous reactions (Myriokefalitakis et al., 2011). Additionally OC shows a good correlation with C$_2$O$_4^{-2}$ that remains constant year-round (R = 0.47, n = 1362, p < 0.001), suggesting involvement of some common emission processes between OC and C$_2$O$_4^{-2}$, such as photochemical and/or heterogeneous reactions (e.g., Huang et al., 2006; Myriokefalitakis et al., 2011). Finally, as expected, the correlation between OC and nss-SO$_4^{-2}$ is considerably higher in summer (winter R = 0.17, n = 272, p < 0.05, summer R = 0.47, n = 327, p < 0.001), when there is intense photochemical activity and significant influence from regional sources due to absence of precipitation.

Finally, the PM$_{2.5}$ mass concentration presents good correlation with NH$_4^+$ and nss-SO$_4^{-2}$ that improves during summer (R = 0.58, n = 303, p < 0.001 and R = 0.66, n = 297, p < 0.001, for summer NH$_4^+$ and nss-SO$_4^{-2}$, respectively), supporting the consistent contribution of secondary inorganic ions to PM$_{2.5}$ mass during the warmest period of the year.

3.3.3. Ionic balance

The ionic balance, expressed as the sum of the equivalent concentration (µeq m^{-3}) ratio of cations to anions, may be used as an indicator for the determination of missing cation and/or anion species in aerosol samples (Mihalopoulos et al., 1997). The measured cations are generally not enough to balance the negative charges of anions; only very few samples (dust transport events) are characterized by an excess of cations, revealing that during the five-year period (with the exception of dust events) fine aerosol fraction is prone to be acidic, in agreement with other Mediterranean studies (e.g., Koulouri et al., 2008; Lonati et al., 2008). In Fig. 5, the two regression lines correspond to dust and non-dust events. For the non-dust samples, the slope of the regression (slope = 1.13, R = 0.77, n = 1267, p < 0.001) suggests a small cation deficit that may be linked to the presence of hydrogen ions (H$^+$) (Tsitouridou and Samara, 1993; Mihalopoulos et al., 1997; Kerminen et al., 2001), not measured by the applied ion chromatography. During dust events, the slope of regression line (slope = 0.94, R = 0.74, n = 210, p < 0.001), indicates that there is some anion deficit which is probably explained by an excess of carbonates (CO$_3^{-2}$) deriving from calcium carbonate (Mihalopoulos et al., 1997). These results are in agreement with findings previously reported by Karageorgos and Rapsomanikis (2007), Theodosi et al. (2011), Pateraki et al. (2008) and Remoundaki et al. (2013) for the area of Athens.

Additional linear regression analysis was performed, in order to understand the relationship between the acid–base balance and the major aerosol components. Given the aforementioned results, carbonate (expressed as the anion deficit) is expected to associate with nss-Ca^{+2}, while H$^+$ (expressed as the cation deficit) should be correlated to nss-SO$_4^{-2}$. The daily values of the cation deficit, calculated as the excess of negative charge (sum of anions minus sum of cations, in µeq m^{-3}), show a moderate correlation with the daily concentrations of nss-SO$_4^{-2}$ (R = 0.39, n = 1058, p < 0.001), illustrating that part of the SO$_4^{-2}$ exists in the acidic form HSO$_4^-$ (Mihalopoulos et al., 1997). On the other hand, the anion deficit (in µeq m^{-3}), corresponding to dust transport from Africa, is very well correlated with nss-Ca^{+2} (R = 0.79, n = 55, p < 0.001), suggesting that CO$_3^{-2}$ is the main missing anion in the fine aerosol fraction during dust events.

3.4. Chemical mass closure

A chemical mass closure exercise was performed for the PM$_{2.5}$ aerosol fraction, accounting for the entire (five-year) sampling period. Masses from filter weighing were checked versus the sum of the masses of the individual chemical components while, as already mentioned in Section 2.4, a classification of all collected samples into dust and non-dust was performed. For reconstructing the PM mass, aerosol is classified into six major components: (i) particulate organic matter (POM), estimated using the OC concentration and a conversion factor of 2.1

Fig. 5. Ionic balance (µeq m^{-3}) for PM$_{2.5}$ during dust and non-dust events at Penteli station, for the period of May 2008–April 2013.

for suburban aerosol, as described in detail by Paraskevopoulou et al. (2014) and references therein; (ii) EC; (iii) sea salt (SS), estimated as the sum of Na^+, Cl^-, Mg^{+2}, $ss-Ca^{+2}$, $ss-SO_4^{-2}$ and $ss-K^+$, assuming that all Na^+, Cl^- and Mg^{+2} are of marine origin (Sciare et al., 2005); (iv) ion mass (IM), as the sum of nss-constituents (NH_4^+, NO_3^-, nss-K^+, nss-SO_4^{-2} and $C_2O_4^{-2}$); (v) water, estimated on the assumption that the water soluble particles in the aerosol are sea salt, NH_4NO_3 and $(NH_4)_2SO_4$ aerosols, according to (Ohta and Okita, 1990); (vi) dust, estimated by a conversion of nss-Ca^{+2}. In particular, as already mentioned in Section 2.2, 100 randomly selected samples from Penteli and Thissio are analyzed by ICP-OES for the determination of major and trace metal concentrations. The correlations between the Al, Fe and nss-Ca^{+2} are studied, since these are considered more representative for transported Saharan dust. The daily concentrations of Al and Fe present a very good correlation (slope = 1.10, R = 0.99, n = 23, p < 0.001 for dust and, slope = 1.25, R = 0.96, n = 30, p < 0.001 for non-dust samples),

revealing common sources for all analyzed samples. Fe is also very well correlated with nss-Ca^{+2} (Fe: slope = 0.55, R = 0.96, n = 23, p < 0.001 for dust and slope = 0.19, R = 0.91, n = 24, p < 0.001 for non-dust samples), suggesting that nss-Ca^{+2} can be used as surrogate to estimate the dust amount. Thus nss-Ca^{+2} concentration is multiplied by a factor of 13.3 and 4.4 to account for dust concentration, during dust and non-dust events respectively; taking into consideration the current estimated correlation between Fe and Ca^{+2} and the content of Fe in earth's crust (Wedepohl, 1995; Guinot et al., 2007 et al., 2007; Guieu et al., 2002).

The gravimetrically and chemically determined mass presented a good correlation (slope = 1.2, R = 0.90, n = 1290, p < 0.001), indicating satisfactory mass balance explanation for the actual $PM_{2.5}$ mass. The results of the mass closure, on a monthly basis, are presented in Fig. 6, where the monthly average reconstructed aerosol mass (columns) is plotted against the gravimetrically measured mass (line), for dust and
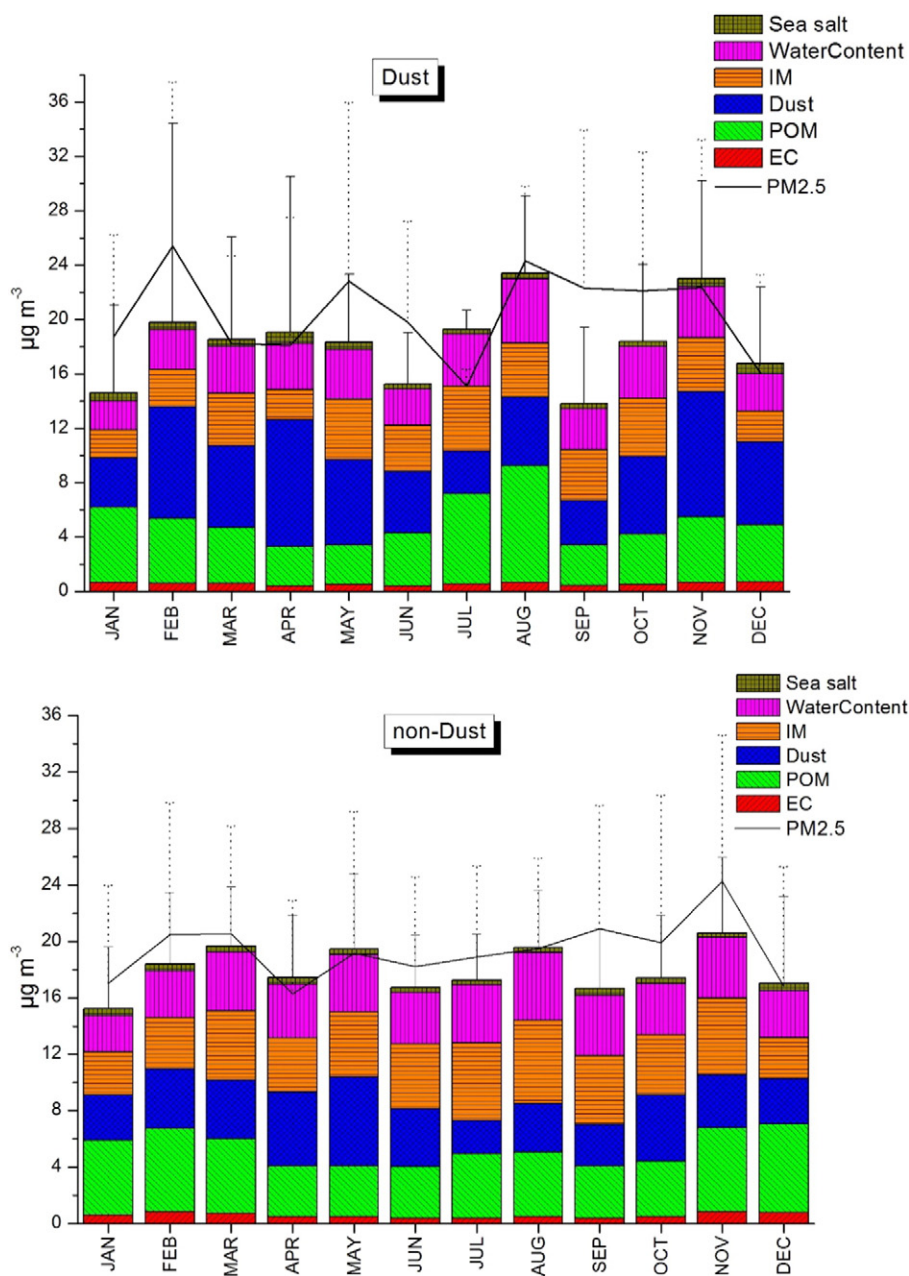

Fig. 6. Mass closure (sea salt, water content, ionic mass, dust, particulate organic matter and elemental carbon) versus measured $PM_{2.5}$, during dust and non-dust events at Penteli station, for the period of May 2008–April 2013.
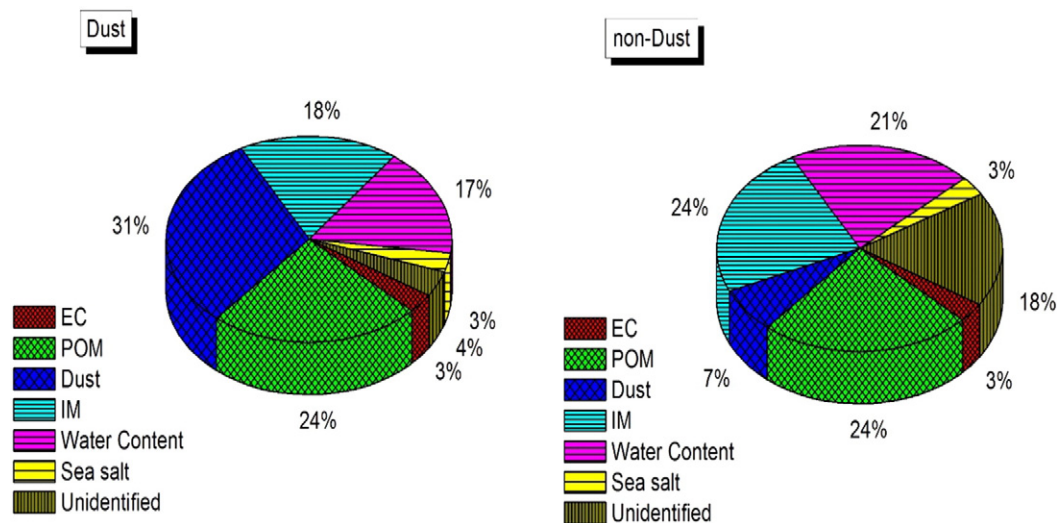
Fig. 7. Average contribution of sea salt, water content, ionic mass, dust, particulate organic matter and elemental carbon to $PM_{2.5}$, during dust and non-dust events at Penteli station, for the period of May 2008–April 2013.

non-dust samples. The sum of the considered categories justifies on average about $96 \pm 11\%$ and $82 \pm 10\%$ of the measured aerosol mass, during the dust and non-dust events, respectively. These values are consistent with other published literature data, reporting average ratios that vary from 73% to 96% (e.g., Hueglin et al., 2005; Lonati et al., 2005; Sillanpää et al., 2006; Viana et al., 2007; Terzi et al., 2010; Cheng et al., 2011; Remoundaki et al., 2013). The unaccounted mass fraction could partly result from the missing metal concentrations. Indeed the chemical mass closure exercise applied on the samples that were analyzed for their content in metals (not shown here), shows that the explained part of the PM mass rises to $93 \pm 9\%$. The rest of the unresolved mass could also be attributed to volatilization losses, measurement artifacts, the uncertainty from rough conversion factor calculation (Li et al., 2010) or systematic errors in chemical analysis (Terzi et al., 2010).

The average contribution of the different chemical types to the $PM_{2.5}$ mass is presented in Fig. 7. During non-dust days, POM and IM account for $24 \pm 6\%$ and $24 \pm 4\%$, respectively, explaining about 44% of the mass. Additionally, the contribution of water in fine aerosol is equally significant in dust ($17 \pm 4\%$) and non-dust ($21 \pm 2\%$) samples, in agreement with water estimation provided in the literature (e.g.,Hueglin et al., 2005; Tsyro, 2005). The categories of SS and EC present low participation in $PM_{2.5}$ (<4%, during both dust and non-dust cases), which is also comparable to values reported for $PM_{2.5}$ by Remoundaki et al. (2013) (SS: 3.6%) in Athens and by Viana et al. (2007) (SS: 1–3%) in

Barcelona. Finally, during dust transport, the contribution of dust increases from $7 \pm 2\%$ to $31 \pm 9\%$.

3.5. Source identification by PCA and PMF

Factor analysis is widely used for source identification and apportionment of particulate matter at sampling sites. The combined use of different factor analysis techniques – PCA and PMF – is here selected, as the most appropriate way to identify and interpret emission sources, and to obtain a quantification of their contributions to the PM mass (Viana et al., 2008b).

3.5.1. Principal component analysis (PCA)

The whole dataset (from May 2008 to April 2013), with OC, EC, major anions and cations for the $PM_{2.5}$ fraction, is first used to perform principal component analysis (PCA) with Varimax rotation, for source identification and apportionment of particulate air pollutants (e.g., Güllü et al., 1998; Sciare et al., 2005; Wang et al., 2005). The PCA indicated the presence of five components in the dataset, each of which explaining at least one unit of variance (Table 3, loadings greater than 0.5 are shown in bold). Each of these factors can be identified as either an emission source, or a chemical interaction (Wu et al., 2013), while their relative contribution reflects differences in emission sources and processes that control the aerosol composition (Putaud et al., 2004).

The five factors together explain up to 85% of the total variance in the dataset. The first factor with high loadings of NH_4^+, SO_4^{+2} and $C_2O_4^{-2}$ can be linked to secondary photochemistry (Sciare et al., 2005). This factor explains up to 34% of the total variance. The second factor accounts for 20% of the variability and shows high loadings for OC, EC and moderate loading of NO_3^-; it can be assigned to anthropogenic sources, since all three variables originate mainly from fuel combustion and traffic. The third factor (13% of the variance) is dominated by Ca^{+2}, which is a typical tracer for mineral material (e.g., Guieu et al., 2002). The forth factor covers an additional 10% of the total variance and may be attributed to biomass burning sources, since it is predominantly influenced by potassium (nss-K^+, tracer for wood burning e.g., Schmidl et al., 2008). Finally, the fifth factor can be attributed to sea salt as it is characterized by enhanced Cl^-.

The results from PCA indicate the dominance of secondary aerosol, soil and fuel combustion sources and are in agreement with the chemical mass closure exercise presented in Section 3.4.

Table 3
PCA, Varimax rotated factor loadings for the fine particle data set from May 2008 to April 2013, in Penteli, Athens.

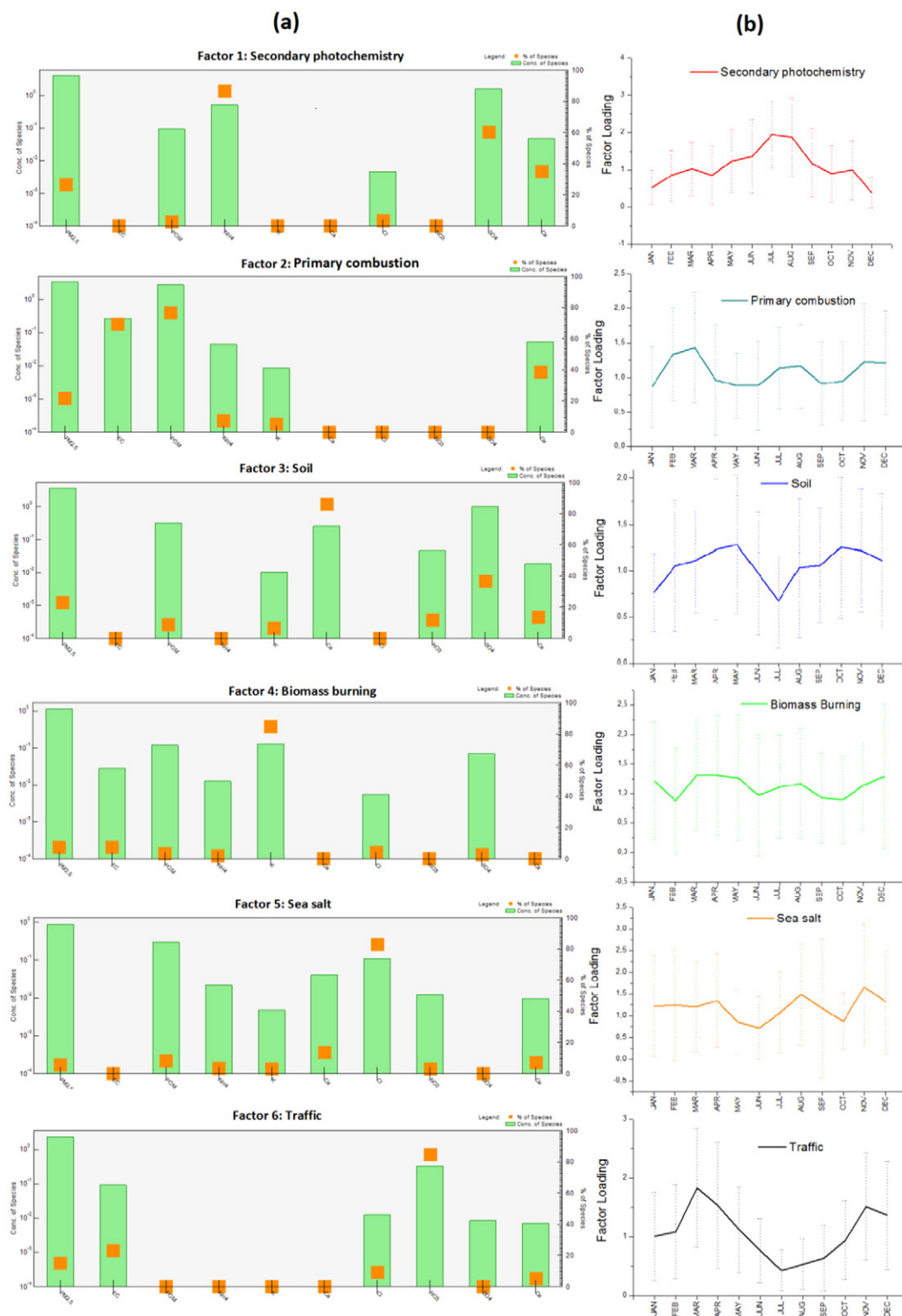|	F1	F2	F3	F4	F5
OC	0.35	**0.81**	0.11	0.00	0.07
EC	0.16	**0.89**	−0.01	0.10	−0.08
NH_4^+	**0.91**	0.06	0.17	0.09	0.02
K^+	0.16	0.11	0.04	**0.98**	−0.02
Ca^{2+}	−0.04	0.00	**−0.96**	−0.05	0.11
Cl^-	0.07	0.05	−0.13	−0.02	**0.97**
NO_3^-	−0.19	**0.66**	−0.44	0.12	0.21
SO_4^{2-}	**0.93**	0.06	−0.05	0.09	−0.05
Ox ($C_2O_4^{-2}$)	**0.71**	0.35	0.00	0.07	0.18
% total variance	33.9	20.0	13.2	9.7	8.2
	Secondary photochemistry	Primary combustion	Soil	Biomass burning	Sea salt

Fig. 8. (a) Source profiles of PM$_{2.5}$ and (b) seasonal variations of factor loadings, according to PMF, at Penteli station, for the period of May 2008–April 2013.

3.5.2. Positive Matrix Factorization (PMF)

For the determination of the number of sources through the PMF analysis, a total of 10 variables (PM$_{2.5}$, EC, POM, NH$_4^+$, K$^+$, Ca^{2+}, Cl$^-$, NO$_3^-$, SO$_4^{-2}$ and C$_2$O$_4^{-2}$ (Ox)) are selected. The size of input matrix is 1223 (samples) × 10 (elements) with more than 80% of data above the detection limit.

After an initial number of runs altering the number of factors between 4 and 8 factors, six factors were found to provide the optimum computed solution of PMF3 for PM$_{2.5}$; taking into account the criteria for the different Q functions and a rational number of factors to characterize distinct source profiles (Norris et al., 2008). The chemical profiles and explained variations for sources assignment are shown
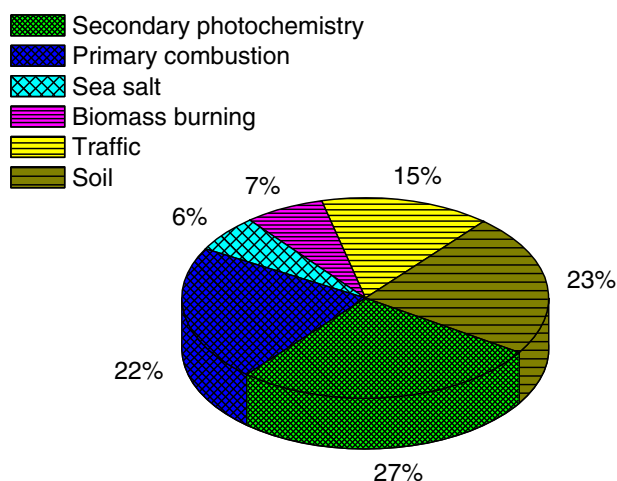
Fig. 9. Average contribution (%) to PM$_{2.5}$ mass of the six identified sources according to PMF, at Penteli station, for the period of May 2008–April 2013.

in Fig. 8, while the resulting source apportionment is presented in Fig. 9. The columns show the mass contribution of species to the factor (in μg m^{-3}) and the spots represent the percentage of the species to the factor.

Factor 1 is highly related to SO$_4^{-2}$ and NH$_4^+$ (Fig. 8a) and can be, hence, assigned to secondary photochemistry. The enhanced photochemistry during summer in the Mediterranean basin favors the formation and preservation of secondary aerosol (Fig. 8b). POM, which is associated to both primary and secondary aerosol, is also found as a component of this source. The estimated source contribution of this factor is 27% (Fig. 9), elucidating the major source of PM$_{2.5}$ in Athens, in agreement with other Mediterranean studies (e.g., Pey et al., 2009; Pandolfi et al., 2011; Mantas et al., 2014).

In the chemical profile of factor 2 a significant contribution is provided by POM, EC and the PM$_{2.5}$ mass (Fig. 8a). This source contributes on average 22% (Fig. 9) and can be ascribed to primary combustion mainly associated to traffic (e.g., Cheng et al., 2013). This factor does not present a profound seasonal signal (Fig. 8b).

Factor 3 is largely influenced by Ca^{2+}, and it represents a soil source from both Sahara long range transport and local soil re-suspension, as it is affected by mixing with inorganic ions (like sulfate and nitrate) and organics or black carbon (Harrison et al., 1997; Norris et al., 2008; Cheng et al., 2014). This factor is characterized by high contributions from Ca^{2+}, SO$_4^{-2}$, oxalate and PM$_{2.5}$ in the chemical profile (Fig. 8a), indicating that the main contributions originate from crustal particles, which are mixed or coated with secondary acids or organics (Perrone et al., 2013). The average contribution of this factor to the PM$_{2.5}$ mass is 23% (Fig. 9), highlighting the role of soil particles also in the fine aerosol fraction (Kassomenos et al., 2014). The seasonality of the factor (spring and fall peaks, Fig. 8b), certifies the strong association with the frequent Saharan dust transport over the Eastern Mediterranean (Gerasopoulos et al., 2006; Kalivitis et al., 2007).

Factor 4 can be associated with biomass burning sources since it is strongly dependent on K$^+$ (Fig. 8a), a characteristic tracer of biomass burning as already discussed in Section 3.5.1. Biomass burning is identified through the presence of noticeable proportions of potassium (nss-K$^+$), POM, SO$_4^{-2}$, NH$_4^+$ and Cl$^-$, while it is worth noting that there is no contribution from NO$_3^-$. This finding suggests that this biomass burning aerosol is freshly emitted near the studied site and has undergone no substantial atmospheric aging (Bressi et al., 2013). The contribution of this factor to the PM$_{2.5}$ mass is on average 7% (Fig. 9), while its seasonal variation shows peaks in spring due to long range transport (Sciare et al., 2008) and in winter when wood burning was selected for domestic heating, mainly during the last two studied years (Fig. 8b).

Factor 5 is associated to sea salt as it is characterized by high contributions from Cl$^-$ and Ca^{2+} in the chemical profile (Fig. 8a). This sea salt profile contains non-negligible concentrations of NO$_3^-$ and SO$_4^{-2}$, which are however not typical of sea-spray aerosols. Consequently, the sea profile seems to be enriched by anthropogenic compounds during their transport to the studied urban background site, in agreement with other reported sites (Kocak et al., 2011; Bressi et al., 2013). The estimated contribution of this source is 6% (Fig. 9).

The aforementioned PMF factors are in agreement with the results from PCA, while in PMF there is an additional sixth factor identified. Observing the high contributions for NO$_3^-$ followed by EC and PM$_{2.5}$, and the relevance of these compounds in the chemical profile (Fig. 8a), factor 6 is identified as the contribution due to traffic. The seasonal cycle of this factor presents minimum values during summer, when the circulation of vehicles is noticeably reduced due to holidays and boundary layer height is significantly increased compared to winter (Fig. 8b). The road traffic source is identified by the presence of characteristic carbonaceous and inorganic materials. The average apportionment of this factor is 15% (Fig. 9) for PM$_{2.5}$, in agreement with findings reported by Pey et al. (2009).

Comparing the acquired PMF results with the available PMF models' bibliography for Athens and other European sites, it is concluded that factor 1 is in agreement with posterior PMF studies that have been performed in the area of Athens for a shorter time period (Mantas et al., 2014). The mineral dust factor (factor 2) accords with previous studies in Athens (Mantas et al., 2014) and Mediterranean basin (Vecchi et al., 2008), which have recorded however lower contributions to fine aerosol masses (<10%). The biomass burning factor (factor 4) is confirmed by posterior reported biomass burning sources in Athens (Karanasiou et al., 2009; Mantas et al., 2014), and other European studies, as well (e.g., Vecchi et al., 2008; Draxler et al., 2009; Dall'Osto et al., 2014). In regards to the marine aerosol factor similar results are reported by Aldabe et al. (2011) for Navarra (North of Spain), while a marine source has been recorded for PM$_{2.5}$ in Athens by Mantas et al. (2014). Finally, the factor dominated by nitrate (factor 6) was reported similarly for Athens by Mantas et al. (2014) and for other urban Mediterranean sites, as well (Kocak et al., 2009; Perrone et al., 2013). It is important to note that the current case PMF analysis has been performed for a long-term period, combined with chemical mass closure exercise and PCA analysis, allowing the deduction of valid conclusions regarding the identification and contribution of fine aerosol sources in the area of Athens that comprises an influential mixture of air pollutants.
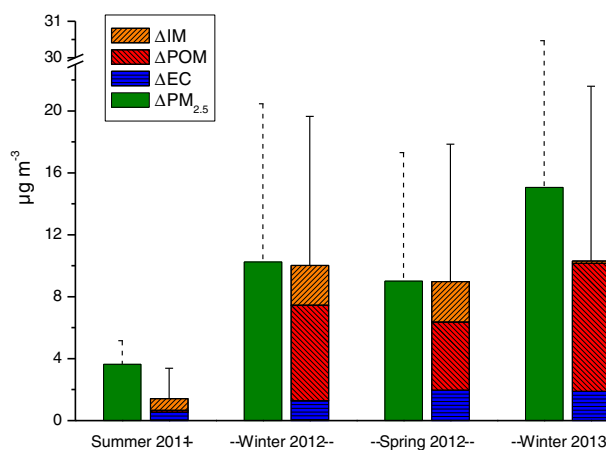

Fig. 10. Relative contribution of local sources (IM, POM and EC) to PM$_{2.5}$ at Thissio station, during seasonal sampling campaigns. ΔPM$_{2.5}$ corresponds to the additional PM$_{2.5}$ mass concentration of the urban site (Thissio) using as reference the urban background site (Penteli).

3.6. Local versus regional contribution to PM$_{2.5}$ masses

Four, short-term sampling campaigns were conducted, simultaneously with Penteli station's sampling, at an urban site in Athens (Thissio), covering 3 different seasons (spring, summer and winter) (Section 2.2). Considering the suburban site at Penteli as urban background, it is feasible to identify and quantify the contribution of the urban sources over Greater Athens area (GAA).

The average masses at Thissio were 33 ± 12 μg m^{-3} and 53 ± 17 μg m^{-3}, for PM$_{2.5}$ and PM$_{10}$, respectively. Comparing the PM$_{2.5}$ masses, the Thissio/Penteli ratio varies from 1.4 in summer to 2.4 in winter, while for PM$_{10}$ the corresponding values are 1.5 and 2.2, respectively. The OC concentrations are 1.1 to 2.9 times higher at Thissio, with an average of 5.6 ± 2.0 μg m^{-3}. For EC there is a more distinct difference between the two sites (2.4 to 4.4 times higher EC concentrations at Thissio), averaging at 0.64 ± 0.22 μg m^{-3}. Similarly, the corresponding Thissio/Penteli ratios for the concentrations of the major ions vary between 1.0–1.7 for NH$_4^+$, 1.2–2.8 for NO$_3^{-1}$ and 1.1–1.8 for SO$_4^{-2}$.

The reconstruction of the weighed masses at the two sampling sites is performed using the aforementioned six categories: POM, Dust, IM, EC, SS and water, in order to investigate the impacts of regional and local aerosol sources, since the suburban site clearly reflects the aerosol background sources, permitting to estimate the contribution of local aerosol emissions at the GAA (Fig. 10). As expected, during summer the concentrations between the two sites do not present significant variation, due to the weather conditions that favor the regional transport and mixing of polluted air masses. The highest additional concentrations at the urban site are observed during winter, highlighting the importance of local sources during the coldest period of the year (Paraskevopoulou et al., 2014). More specifically, during winter time, EC contributes from about 13% (during winter 2012) to 18% (during winter 2013) while, IM contributes from about 2% (during winter 2013) to 26% (during winter 2012) to the additional concentrations at the urban station.

Using the suburban site as a reference, it is estimated that local sources dominate during the coldest period (Paraskevopoulou et al., 2014); with the relative contribution of local EC, IM and POM being 52–56% in winter, while during the warmest period, about 89% of EC, IM and POM is regional. POM appears to be the main constituent of the additional local aerosol that is present at the urban site, in agreement with results reported by Theodosi et al. (2011) for Athens, since its additional urban contribution is calculated from about 49% (during spring 2012) to 80% (during winter 2013). In addition, from winter 2012 to winter 2013 the contribution of POM to the additional local aerosol mass is increased by 30%, reflecting the impact of wood combustion (dominant fuel for domestic heating) to air quality in Athens, which massively started in winter 2013.

4. Conclusions

Five-year sampling was conducted at a suburban site in Athens, resulting in the collection of 1510 daily fine aerosol samples, that were chemically analyzed for their content in OC, EC, major anions and cations and, major and trace metals (on a selective number of samples). Subsequently, the chemical properties were utilized for chemical mass closure exercise, PCA analysis and PMF model application, in order to identify and quantify the contribution of fine aerosol sources in the studied area. Simultaneous seasonal sampling campaigns were also conducted at an urban station, enabling the estimation of the relative contribution of local and regional urban aerosol emissions at GAA.

It is important to note that the current PMF analysis has been performed for a long-term period, combined with chemical mass closure exercise and PCA analysis, allowing the deduction of valid conclusions regarding the identification and contribution of fine aerosol sources in the area of Athens that comprises an influential mixture of air pollutants. This first long-term work, constitutes a rare study of aerosol emissions in GAA.

The main conclusions emerging from this research are presented below:

– The 24-h concentrations of PM$_{2.5}$, PM$_{2.5–10}$ and PM$_{10}$ at the suburban site at Penteli vary from 1.2 to 65.8 μg m^{-3}, 0.2 to 213.1 μg m^{-3} and 3.0 to 329.7 μg m^{-3}, respectively, with an overall average of 20 ± 11 μg m^{-3} for PM$_{2.5}$, 17 ± 13 μg m^{-3} for PM$_{2.5–10}$ and 35 ± 20 μg m^{-3} for PM$_{10}$. The inter-annual trend of PM masses reveals a decrease of ambient aerosol masses through the studied 5-year period, which is attributed to measures adopted during the last decades but also due to further reduction of anthropogenic emissions since the economic recession originating in Greece.

– A detailed analysis of the ion mass fraction reveals that nss-SO$_4^{-2}$ is the prevailing specie and, NO$_3^-$ and NH$_4^+$ contribute to a lesser extent. The contribution of nss-SO$_4^{-2}$ to IM is 63 ± 7% and 52 ± 14% for non-dust and dust samples, respectively, while with regards to the total PM$_{2.5}$ mass, nss-SO$_4^{-2}$ presents an average contribution of 15 ± 4% for the five-year period.

– The inter-annual trend of nss-SO$_4^{-2}$ follows the decreasing trend of PM masses. These lower levels of in-situ measured pollutants as derived from detail chemical composition data, are reported for the first time in the area of Athens, highlighting the effects of the economic recession in Greece. - The chemical mass closure exercise justifies on average about 96 ± 11% and 82 ± 10% of the measured aerosol mass, during the dust and non-dust events, respectively. The unaccounted mass fraction could partly result from the missing metals concentrations. During non-dust days, POM and IM contribute 24 ± 6% and 24 ± 4%, respectively, explaining about 44% of the mass. Additionally, the contribution of water in fine aerosol is equally significant (dust: 17 ± 4%, non-dust: 21 ± 2%) in dust and non-dust samples. The categories of SS and EC present low participation in PM$_{2.5}$ (<4%, during both dust and non-dust cases) while, during dust transport, the contribution of dust increases from a background of 7 ± 2% to 31 ± 9%.

– PCA and PMF revealed five common aerosol sources of fine aerosol in the suburban site: secondary photochemistry, fuel combustion, soil, biomass burning and sea salt; while an additional sixth factor of traffic is identified by PMF model, confirming the dominance of secondary aerosol, soil and fuel combustion sources that are presumed by the chemical mass closure exercise.

– Considering the suburban site at Penteli as a reference, the contribution of the urban sources is quantified at the urban site of Thissio, during seasonal sampling campaigns. During summer, the concentrations between the two sites do not present significant variation, due to the weather conditions that favor the regional transport and mixing of polluted air masses. The highest additional concentrations at the urban site are observed during winter, highlighting the prevailing local sources during the coldest period of the year. POM appears to be the main constituent of the additional local aerosol that is present at the urban site. More specifically, from winter 2012 to winter 2013 the contribution of POM to the additional local aerosol increases by 30%, reflecting the impact of the economic recession on the air quality of Athens, since during the last studied winters, wood combustion dominated used fuels for domestic heating.

Program: Heracleitus II. Investing in knowledge society through the European Social Fund.

References

Aldabe, J., Elustondo, D., Santamaria, C., Lasheras, E., Pandolfi, M., Alastuey, A., Querol, X., Santamaria, J.M., 2011. Chemical characterisation and source apportionment of PM$_{2.5}$ and PM$_{10}$ at rural, urban and traffic sites in Navarra (North of Spain). Atmos. Res. 102, 191–205.

Bardouki, H., Liakakou, H., Economou, C., Sciare, J., Smolik, J., Zdimal, V., Eleftheriadis, K., Lazaridis, M., Dye, C., Mihalopoulos, N., 2003. Chemical composition of size-resolved atmospheric aerosols in the Eastern Mediterranean during summer and winter. Atmos. Environ. 37, 195–208.

Beddows, D.C.S., Donovan, R.J., Harrison, R.M., Heal, M.R., Kinnersley, R.P., King, M.D., Nicholson, D.H., Thompson, K.C., 2004. Correlations in the chemical composition of rural background atmospheric aerosol in the UK determined in real time using time-of-flight mass spectrometry. J. Environ. Monit. 6, 124–133.

Belis, C.A., Karagulian, F., Larsen, B.R., Hopke, P.K., 2013. Critical review and meta-analysis of ambient particulate matter source apportionment using receptor models in Europe. Atmos. Environ. 69, 94–108.

Bell, M.L., Ebisu, K., Peng, R.D., Samet, J.M., Dominici, F., 2009. Hospital admissions and chemical composition of fine particle air pollution. Am. J. Respir. Crit. Care Med. 179, 1115–1120.

Blifford Jr., I.H., Meeker, G.O., 1967. A factor analysis model of large scale pollution. Atmos. Environ. 1, 147–157.

Bougiatioti, A., Zarmpas, P., Koulouri, E., Antoniou, M., Theodosi, C., Kouvarakis, G., Saarikoski, S., Makela, T., Hillamo, R., Mihalopoulos, N., 2013. Organic, elemental and water-soluble organic carbon in size segregated aerosols, in the marine boundary layer of the Eastern Mediterranean. Atmos. Environ. 64, 251–262.

Bressi, M., Sciare, J., Ghersi, V., Mihalopoulos, N., Petit, J.E., Nicolas, J.B., Moukhtar, S., Rosso, A., Feron, A., Bonnaire, N., Poulakis, E., Theodosi, C., 2013. Sources and geographical origins of fine aerosols in Paris (France). Atmos. Chem. Phys. Discuss. 13, 33237–33309.

Cavalli, F., Viana, M., Yttri, K.E., Genberg, J., Putaud, J.P., 2010. Toward a standardised thermal-optical protocol for measuring atmospheric organic and elemental carbon: the EUSAAR protocol. Atmos. Meas. Tech. 3, 79–89.

Chaloulakou, A., Kassomenos, P., Grivas, G., Spyrellis, N., 2005. Particulate matter and black smoke concentration levels in central Athens, Greece. Environ. Int. 31, 651–659.

Cheng, Y., He, K.-B., Duan, F.-K., Zheng, M., Du, Z.-Y., Ma, Y.-L., Tan, J.-H., 2011. Ambient organic carbon to elemental carbon ratios: influences of the measurement methods and implications. Atmos. Environ. 45, 2060–2066.

Cheng, Y., Lee, S., Gu, Z., Ho, K., Zhang, Y., Huang, Y., Chow, J.C., Watson, J.G., Cao, J., Zhang, R., 2013. PM$_{2.5}$ and P M$_{10-2.5}$ chemical composition and source apportionment near a Hong Kong roadway. Particuology 18, 96–104.

Cheng, T., Gu, X., Wu, Y., Chen, H., 2014. Effects of atmospheric water on the optical properties of soot aerosols with different mixing states. J. Quant. Spectrosc. Radiat. Transf. 147, 196–206.

Cusack, M., Alastuey, A., Pérez, N., Pey, J., Querol, X., 2012. Trends of particulate matter (PM$_{2.5}$) and chemical composition at a regional background site in the Western Mediterranean over the last nine years (2002–2010). Atmos. Chem. Phys. 12, 8341–8357.

Daher, N., Saliba, N.A., Shihadeh, A.L., Jaafar, M., Baalbaki, R., Sioutas, C., 2013. Chemical composition of size-resolved particulate matter at near-freeway and urban background sites in the greater Beirut area. Atmos. Environ. 80, 96–106.

Dall'Osto, M., Hellebust, S., Healy, R.M., Connor, I.P., Kourtchev, I., Sodeau, J.R., Ovadnevaite, J., Ceburnis, D., O'Dowd, C.D., Wenger, J.C., 2014. Apportionment of urban aerosol sources in Cork (Ireland) by synergistic measurement techniques. Sci. Total Environ. 493, 197–208.

Dockery, D.W., Pope, C.A., 1994. Acute respiratory effects of particulate air pollution. Annu. Rev. Public Health 15, 107–132.

Draxler, R.R., Stunder, B., Rolph, G.D., Talylor, A.D., 2009. Hysplit 4 User's Guide. NOAA Air Resources Laboratory, Silver Spring, MD, USA.

Engelhart, G.J., Hildebrandt, L., Kostenidou, E., Mihalopoulos, N., Donahue, N.M., Pandis, S.N., 2011. Water content of aged aerosol. Atmos. Chem. Phys. 11, 21653–21681.

Gerasopoulos, E., Kouvarakis, G., Babasakalis, P., Vrekoussis, M., Putaud, J.P., Mihalopoulos, N., 2006. Origin and variability of particulate matter (PM$_{10}$) mass concentrations over the Eastern Mediterranean. Atmos. Environ. 40, 4679–4690.

Gerasopoulos, E., Amiridis, V., Kazadzis, S., Kokkalis, P., Eleftheratos, K., Andreae, M.O., Andreae, T.W., El-Askary, H., Zerefos, C.S., 2011. Three-year ground based measurements of aerosol optical depth over the Eastern Mediterranean: the urban environment of Athens. Atmos. Chem. Phys. 11, 2145–2159.

Guieu, C., Loÿe-Pilot, M.D., Ridame, C., Thomas, C., 2002. Chemical characterization of the Saharan dust end-member: some biogeochemical implications for the western Mediterranean Sea. J. Geophys. Res. Atmos. 107 (ACH 5-1-ACH 5–11).

Guinot, B., Cachier, H., Oikonomou, K., 2007. Geochemical perspectives from a new aerosol chemical mass closure. Atmos. Chem. Phys. 7, 1657–1670.

Güllü, G.H., Ölmez, I., Aygün, S., Tuncel, G., 1998. Atmospheric trace element concentrations over the Eastern Mediterranean Sea: factors affecting temporal variability. J. Geophys. Res. Atmos. 103, 21943–21954.

Harrison, R.M., Pio, C.A., 1983. Size-differentiated composition of inorganic atmospheric aerosols of both marine and polluted continental origin. Atmos. Environ. 17, 1733–1738.

Harrison, R.M., Smith, D.J.T., Piou, C.A., Castro, L.M., 1997. Comparative receptor modelling study of airborne particulate pollutants in Birmingham (United Kingdom), Coimbra (Portugal) and Lahore (Pakistan). Atmos. Environ. 31, 3309–3321.

Ho, K.F., Lee, S.C., Cao, J.J., Chow, J.C., Watson, J.G., Chan, C.K., 2006. Seasonal variations and mass closure analysis of particulate matter in Hong Kong. Sci. Total Environ. 355, 276–287.

Huang, X.-F., Yu, J.Z., He, L.-Y., Yuan, Z., 2006. Water-soluble organic carbon and oxalate in aerosols at a coastal urban site in China: size distribution characteristics, sources, and formation mechanisms. J. Geophys. Res. Atmos. 111, D22212.

Hueglin, C., Gehrig, R., Baltensperger, U., Gysel, M., Monn, C., Vonmont, H., 2005. Chemical characterisation of PM$_{2.5}$, PM$_{10}$ and coarse particles at urban, near-city and rural sites in Switzerland. Atmos. Environ. 39, 637–651.

Kalivitis, N., Gerasopoulos, E., Vrekoussis, M., Kouvarakis, G., Kubilay, N., Hatzianastassiou, N., Vardavas, I., Mihalopoulos, N., 2007. Dust transport over the Eastern Mediterranean derived from total ozone mapping spectrometer, aerosol robotic network, and surface measurements. J. Geophys. Res. Atmos. 112, D03202.

Kanakidou, M., Seinfeld, J.H., Pandis, S.N., Barnes, I., Dentener, F.J., Facchini, M.C., Van Dingenen, R., Ervens, B., Nenes, A., Nielsen, C.J., Swietlicki, E., Putaud, J.P., Balkanski, Y., Fuzzi, S., Horth, J., Moortgat, G.K., Winterhalter, R., Myhre, C.E.L., Tsigaridis, K., Vignati, E., Stephanou, E.G., Wilson, J., 2005. Organic aerosol and global climate modelling: a review. Atmos. Chem. Phys. 5, 1053–1123.

Kanakidou, M., Mihalopoulos, N., Kindap, T., Im, U., Vrekoussis, M., Gerasopoulos, E., Dermitzaki, E., Unal, A., Kocak, M., Markakis, K., Melas, D., Kouvarakis, G., Youssef, A.F., Richter, A., Hatzianastassiou, N., Hilboll, A., Ebojie, F., Wittrock, F., von Savigny, C., Burrows, J.P., Ladstaetter-Weissenmayer, A., Moubasher, H., 2011. Megacities as hot spots of air pollution in the East Mediterranean. Atmos. Environ. 45, 1223–1235.

Karageorgos, E.T., Rapsomanikis, S., 2007. Chemical characterization of the inorganic fraction of aerosols and mechanisms of the neutralization of atmospheric acidity in Athens, Greece. Atmos. Chem. Phys. 7, 3015–3033.

Karanasiou, A.A., Siskos, P.A., Eleftheriadis, K., 2009. Assessment of source apportionment by positive matrix factorization analysis on fine and coarse urban aerosol size fractions. Atmos. Environ. 43, 3385–3395.

Kassomenos, P.A., Vardoulakis, S., Chaloulakou, A., Paschalidou, A.K., Grivas, G., Borge, R., Lumbreras, J., 2014. Study of PM$_{10}$ and PM$_{2.5}$ levels in three European cities: analysis of intra and inter urban variations. Atmos. Environ. 87, 153–163.

Kerminen, V.-M., Hillamo, R., Teinilä, K., Pakkanen, T., Allegrini, I., Sparapani, R., 2001. Ion balances of size-resolved tropospheric aerosol samples: implications for the acidity and atmospheric processing of aerosols. Atmos. Environ. 35, 5255–5265.

Kocak, M., Mihalopoulos, N., Kubilay, N., 2009. Origin and source regions of PM$_{10}$ in the Eastern Mediterranean atmosphere. Atmos. Res. 92, 464–474.

Kocak, M., Theodosi, C., Zarmpas, P., Im, U., Bougiatioti, A., Yenigun, O., Mihalopoulos, N., 2011. Particulate matter (PM$_{10}$) in Istanbul: origin, source areas and potential impact on surrounding regions. Atmos. Environ. 45, 6891–6900.

Koulouri, E., Saarikoski, S., Theodosi, C., Markaki, Z., Gerasopoulos, E., Kouvarakis, G., Makela, T., Hillamo, R., Mihalopoulos, N., 2008. Chemical composition and sources of fine and coarse aerosol particles in the Eastern Mediterranean. Atmos. Environ. 42, 6542–6550.

Li, N., Sioutas, C., Cho, A., Schmitz, D., Misra, C., Sempf, J., Wang, M., Oberley, T., Froines, J., Nel, A., 2003. Ultrafine particulate pollutants induce oxidative stress and mitochondrial damage. Environ. Health Perspect. 111, 455–460.

Li, L., Wang, W., Feng, J., Zhang, D., Li, H., Gu, Z., Wang, B., Sheng, G., Fu, J., 2010. Composition, source, mass closure of PM$_{2.5}$ aerosols for four forests in eastern China. J. Environ. Sci. 22, 405–412.

Lonati, G., Giugliano, M., Butelli, P., Romele, L., Tardivo, R., 2005. Major chemical components of PM$_{2.5}$ in Milan (Italy). Atmos. Environ. 39, 1925–1934.

Lonati, G., Giugliano, M., Ozgen, S., 2008. Primary and secondary components of PM$_{2.5}$ in Milan (Italy). Environ. Int. 34, 665–670.

Mantas, E., Remoundaki, E., Halari, I., Kassomenos, P., Theodosi, C., Hatzikioseyian, A., Mihalopoulos, N., 2014. Mass closure and source apportionment of PM$_{2.5}$ by positive matrix factorization analysis in urban Mediterranean environment. Atmos. Environ. 94, 154–163.

Mariani, R.L., de Mello, W.Z., 2007. PM$_{2.5-10}$, PM$_{2.5}$ and associated water-soluble inorganic species at a coastal urban site in the metropolitan region of Rio de Janeiro. Atmos. Environ. 41, 2887–2892.

Melas, D., Ziomas, I., Klemm, O., Zerefos, C.S., 1998. Flow dynamics in Athens area under moderate large-scale winds. Atmos. Environ. 32, 2209–2222.

Mihalopoulos, N., Stephanou, E., Kanakidou, M., Pilitsidis, S., Bousquet, P., 1997. Tropospheric aerosol ionic composition in the Eastern Mediterranean region. Tellus Ser. B Chem. Phys. Meteorol. 49.

Mirante, F., Salvador, P., Pio, C., Alves, C., Artinano, B., Caseiro, A., Revuelta, M.A., 2014. Size fractionated aerosol composition at roadside and background environments in the Madrid urban atmosphere. Atmos. Res. 138, 278–292.

Myriokefalitakis, S., Tsigaridis, K., Mihalopoulos, N., Sciare, J., Nenes, A., Kawamura, K., Segers, A., Kanakidou, M., 2011. In-cloud oxalate formation in the global troposphere: a 3-D modeling study. Atmos. Chem. Phys. 11, 5761–5782.

Norris, G., Vedantham, R., Wade, K., Brown, S., Prouty, J., Foley, C., Martin, L., 2008. EPA Positive Matrix Factorization (PMF) 3.0 Fundamentals & User Guide. U.S. Environmental Protection Agency.

Ohta, S., Okita, T., 1990. A chemical characterization of atmospheric aerosol in Sapporo. Atmos. Environ., Part A 24, 815–822.

Ostro, B., Broadwin, R., Green, S., Feng, W.Y., Lipsett, M., 2006. Fine particulate air pollution and mortality in nine California counties: results from CALFINE. Environ. Health Perspect. 114, 29–33.

Ozturk, F., Zararsiz, A., Dutkiewicz, V.A., Husain, L., Hopke, P.K., Tuncel, G., 2012. Temporal variations and sources of Eastern Mediterranean aerosols based on a 9-year observation. Atmos. Environ. 61, 463–475.

Paatero, P., 1997. Least squares formulation of robust non-negative factor analysis. Chemom. Intell. Lab. Syst. 37, 23–35.

Paatero, P., Hopke, P.K., 2003. Discarding or downweighting high-noise variables in factor analytic models. Anal. Chim. Acta 490, 277–289.

Pandolfi, M., Gonzalez-Castanedo, Y., Alastuey, A.S., Rosa, J., Mantilla, E., Campa, A.S., Querol, X., Pey, J., Amato, F., Moreno, T., 2011. Source apportionment of PM$_{10}$ and PM$_{2.5}$ at multiple sites in the strait of Gibraltar by PMF: impact of shipping emissions. Environ. Sci. Pollut. Res. 18, 260–269.

Paraskevopoulou, D., Liakakou, E., Gerasopoulos, E., Theodosi, C., Mihalopoulos, N., 2014. Long term characterization of organic and elemental carbon in the PM$_{2.5}$ fraction: the case of Athens, Greece. Atmos. Chem. Phys. 14, 13313–13325. http://dx.doi.org/10.5194/acp-14-13313-2014.

Park, S.S., Ondov, J.M., Harrison, D., Nair, N.P., 2005. Seasonal and shorter-term variations in particulate atmospheric nitrate in Baltimore. Atmos. Environ. 39, 2011–2020.

Pateraki, S., Maggos, T., Michopoulos, J., Flocas, H.A., Asimakopoulos, D.N., Vasilakos, C., 2008. Ions species size distribution in particulate matter associated with VOCs and meteorological conditions over an urban region. Chemosphere 72 (3), 496–503. http://dx.doi.org/10.1016/j.chemosphere.2008.02.061 (Jun, Epub 2008 Apr 25).

Pateraki, S., Assimakopoulos, V.D., Bougiatioti, A., Kouvarakis, G., Mihalopoulos, N., Vasilakos, C., 2012. Carbonaceous and ionic compositional patterns of fine particles over an urban Mediterranean area. Sci. Total Environ. 424, 251–263.

Pennanen, A.S., Sillanpaa, M., Hillamo, R., Quass, U., John, A.C., Branis, M., Hunova, I., Meliefste, K., Janssen, N.A.H., Koskentalo, T., Castano-Vinyals, G., Bouso, L., Chalbot, M.C., Kavouras, I.G., Salonen, R.O., 2007. Performance of a high-volume cascade impactor in six European urban environments: mass measurement and chemical characterization of size-segregated particulate samples. Sci. Total Environ. 374, 297–310.

Perrone, M.R., Piazzalunga, A., Prato, M., Carofalo, I., 2011. Composition of fine and coarse particles in a coastal site of the central Mediterranean: carbonaceous species contributions. Atmos. Environ. 45, 7470–7477.

Perrone, M.R., Becagli, S., Garcia Orza, J.A., Vecchi, R., Dinoi, A., Udisti, R., Cabello, M., 2013. The impact of long-range-transport on PM$_1$ and PM$_{2.5}$ at a Central Mediterranean site. Atmos. Environ. 71, 176–186.

Pey, J., Perez, N., Castillo, S., Viana, M., Moreno, T., Pandolfi, M., Lopez-Sebastian, J.M., Alastuey, A., Querol, X., 2009. Geochemistry of regional background aerosols in the Western Mediterranean. Atmos. Res. 94, 422–435.

Pio, C.A., Legrand, M., Oliveira, T., Afonso, J., Santos, C., Caseiro, A., Fialho, P., Barata, F., Puxbaum, H., Sanchez-Ochoa, A., Kasper-Giebl, A., Gelencsér, A., Preunkert, S., Schock, M., 2007. Climatology of aerosol composition (organic versus inorganic) at nonurban sites on a west–east transect across Europe. J. Geophys. Res. Atmos. 112, D23S02.

Polissar, A.V., Hopke, P.K., Paatero, P., Malm, W.C., Sisler, J.F., 1998. Atmospheric aerosol over Alaska: 2. Elemental composition and sources. J. Geophys. Res. Atmos. 103, 19045–19057.

Putaud, J.-P., Raes, F., Van Dingenen, R., Bruggemann, E., Facchini, M.C., Decesari, S., Fuzzi, S., Gehrig, R., Huglin, C., Laj, P., Lorbeer, G., Maenhaut, W., Mihalopoulos, N., Muller, K., Querol, X., Rodriguez, S., Schneider, J., Spindler, G., Brink, H.T., Torseth, K., Wiedensohler, A., 2004. A European aerosol phenomenologyβ€"2: chemical characteristics of particulate matter at kerbside, urban, rural and background sites in Europe. Atmos. Environ. 38, 2579–2595.

Putaud, J.P., Van Dingenen, R., Alastuey, A., Bauer, H., Birmili, W., Cyrys, J., Flentje, H., Fuzzi, S., Gehrig, R., Hansson, H.C., Harrison, R.M., Herrmann, H., Hitzenberger, R., Huglin, C., Jones, A.M., Kasper-Giebl, A., Kiss, G., Kousa, A., Kuhlbusch, T.A.J., Loschau, G., Maenhaut, W., Molnar, A., Moreno, T., Pekkanen, J., Perrino, C., Pitz, M., Puxbaum, H., Querol, X., Rodriguez, S., Salma, I., Schwarz, J., Smolik, J., Schneider, J., Spindler, G., ten Brink, H., Tursic, J., Viana, M., Wiedensohler, A., Raes, F., 2010. A European aerosol phenomenology β€"3: Physical and chemical characteristics of particulate matter from 60 rural, urban, and kerbside sites across Europe. Atmos. Environ. 44, 1308–1320.

Querol, X., Alastuey, A., Ruiz, C.R., Artinano, B., Hansson, H.C., Harrison, R.M., Buringh, E., ten Brink, H.M., Lutz, M., Bruckmann, P., Straehl, P., Schneider, J., 2004. Speciation and origin of PM$_{10}$ and PM$_{2.5}$ in selected European cities. Atmos. Environ. 38, 6547–6555.

Remoundaki, E., Kassomenos, P., Mantas, E., Mihalopoulos, N., Tsezos, M., 2013. Composition and mass closure of PM$_{2.5}$ in urban environment (Athens, Greece). Aerosol Air Qual. Res. 13, 72–82.

Saffari, A., Daher, N., Samara, C., Voutsa, D., Kouras, A., Manoli, E., Karagkiozidou, O., Vlachokostas, C., Moussiopoulos, N., Shafer, M.M., Schauer, J.J., Sioutas, C., 2013. Increased biomass burning Due to the economic crisis in Greece and its adverse impact on wintertime air quality in Thessaloniki. Environ. Sci. Technol. 47, 13313–13320.

Salma, I., Balásházy, I., Winkler-Heil, R., Hofmann, W., Záray, G., 2002. Effect of particle mass size distribution on the deposition of aerosols in the human respiratory system. J. Aerosol Sci. 33, 119–132.

Schmidl, C., Marr, I.L., Caseiro, A., Kotianova, P., Berner, A., Bauer, H., Kasper-Giebl, A., Puxbaum, H., 2008. Chemical characterisation of fine particle emissions from wood stove combustion of common woods growing in mid-European Alpine regions. Atmos. Environ. 42, 126–141.

Sciare, J., Oikonomou, K., Cachier, H., Mihalopoulos, N., Andreae, M.O., Maenhaut, W., Sarda-Esteve, R., 2005. Aerosol mass closure and reconstruction of the light scattering coefficient over the Eastern Mediterranean Sea during the MINOS campaign. Atmos. Chem. Phys. 5, 2253–2265.

Sciare, J., Oikonomou, K., Favez, O., Liakakou, E., Markaki, Z., Cachier, H., Mihalopoulos, N., 2008. Long-term measurements of carbonaceous aerosols in the Eastern Mediterranean: evidence of long-range transport of biomass burning. Atmos. Chem. Phys. 8, 5551–5563.

Seinfeld, J.H., Pandis, S.N., 1998. Atmopseric Chemistry and Physics: From Air Pollution to Climate Change. Wiley, New York.

Sillanpää, M., Hillamo, R., Saarikoski, S., Frey, A., Pennanen, A., Makkonen, U., Spolnik, Z., Van Grieken, R., Braniš, M., Brunekreef, B., Chalbot, M.-C., Kuhlbusch, T., Sunyer, J., Kerminen, V.-M., Kulmala, M., Salonen, R.O., 2006. Chemical composition and mass closure of particulate matter at six urban sites in Europe. Atmos. Environ. 40 (Suppl. 2), 212–223.

Siskos, P.A., Bakeas, E.B., Lioli, I., Smirnioudi, V.N., Koutrakis, P., 2001. Chemical characterization of PM$_{2.5}$ aerosols in Athens-Greece. Environ. Technol. 22, 687–695.

Terzi, E., Argyropoulos, G., Bougatioti, A., Mihalopoulos, N., Nikolaou, K., Samara, C., 2010. Chemical composition and mass closure of ambient PM$_{10}$ at urban sites. Atmos. Environ. 44, 2231–2239.

Theodosi, C., Markaki, Z., Tselepides, A., Mihalopoulos, N., 2010. The significance of atmospheric inputs of soluble and particulate major and trace metals to the Eastern Mediterranean seawater. Mar. Chem. 120, 154–163.

Theodosi, C., Grivas, G., Zarmpas, P., Chaloulakou, A., Mihalopoulos, N., 2011. Mass and chemical composition of size-segregated aerosols (PM$_1$, PM$_{2.5}$, PM$_{10}$) over Athens, Greece: local versus regional sources. Atmos. Chem. Phys. 11, 11895–11911.

Titos, G., Lyamani, H., Pandolfi, M., Alastuey, A., Alados-Arboledas, L., 2014. Identification of fine (PM$_1$) and coarse (PM$_{10-1}$) sources of particulate matter in an urban environment. Atmos. Environ. 89, 593–602.

Tsitouridou, R., Samara, C., 1993. First results of acidic and alkaline constituents determination in air particulates of Thessaloniki, Greece. Atmos. Environ. Part B 27, 313–319.

Tsyro, S.G., 2005. To what extent can aerosol water explain the discrepancy between model calculated and gravimetric PM$_{10}$ and PM$_{2.5}$? Atmos. Chem. Phys. 5, 515–532.

Vecchi, R., Chiari, M., D'Alessandro, A., Fermo, P., Lucarelli, F., Mazzei, F., Nava, S., Piazzalunga, A., Prati, P., Silvani, F., Valli, G., 2008. A mass closure and PMF source apportionment study on the sub-micron sized aerosol fraction at urban sites in Italy. Atmos. Environ. 42, 2240–2253.

Viana, M., Maenhaut, W., Chi, X., Querol, X., Alastuey, A., 2007. Comparative chemical mass closure of fine and coarse aerosols at two sites in south and west Europe: implications for EU air pollution policies. Atmos. Environ. 41, 315–326.

Viana, M., Kuhlbusch, T.A.J., Querol, X., Alastuey, A., Harrison, R.M., Hopke, P.K., Winiwarter, W., Vallius, M., Szidat, S., Prévôt, A.S.H., Hueglin, C., Bloemen, H., Wåhlin, P., Vecchi, R., Miranda, A.I., Kasper-Giebl, A., Maenhaut, W., Hitzenberger, R., 2008a. Source apportionment of particulate matter in Europe: a review of methods and results. J. Aerosol Sci. 39, 827–849.

Viana, M., Pandolfi, M., Minguillón, M.C., Querol, X., Alastuey, A., Monfort, E., Celades, I., 2008b. Inter-comparison of receptor models for PM source apportionment: case study in an industrial area. Atmos. Environ. 42, 3820–3832.

Vrekoussis, M., Richter, A., Hilboll, A., Burrows, J.P., Gerasopoulos, E., Lelieveld, J., Barrie, L., Zerefos, C., Mihalopoulos, N., 2013. Economic crisis detected from space: air quality observations over Athens/Greece. Geophys. Res. Lett. 40, 458–463.

Wang, H., Kawamura, K., Shooter, D., 2005. Carbonaceous and ionic components in wintertime atmospheric aerosols from two New Zealand cities: implications for solid fuel combustion. Atmos. Environ. 39, 5865–5875.

Wedepohl, H.K., 1995. The composition of continental crust. Geochim. Cosmochim. Acta 59, 1217–1232.

Wu, G., Du, X., Wu, X., Fu, X., Kong, S., Chen, J., Wang, Z., Bai, Z., 2013. Chemical composition, mass closure and sources of atmospheric PM$_{10}$ from industrial sites in Shenzhen, China. J. Environ. Sci. 25, 1626–1635.

Zhang, Y., Obrist, D., Zielinska, B., Gertler, A., 2013. Particulate emissions from different types of biomass burning. Atmos. Environ. 72, 27–35.